



TAMPERE UNIVERSITY OF TECHNOLOGY

Rizwan Fazal

Implementation of Communication Receivers as Multi-Processor Software

Master of Science Thesis

Thesis Supervisors: Prof. Jari Nurmi
Asst. Prof. Tapani Ahonen

Examiners and topic approved in the faculty council of the Faculty of Computing and Electrical Engineering on May 8, 2013.

PREFACE

This thesis work has been completed in the Department of Electronics and Communications Engineering at Tampere University of Technology to pursue Masters of Science (MSc) degree in the program of Information Technology.

I would like to thank my supervisor Professor Jari Nurmi for his kind support and guidance throughout my research work in the department. I am also grateful to my co-supervisor Assistant Professor Tapani Ahonen for sharing his expertise and knowledge to me besides his so friendly behavior which I really appreciate. I am also thankful to my research group colleagues Fabio Garzia, Roberto Airoidi and Waqar Hussain for their technical support and guidance.

I would like to thank my parents Baghdad Hussain Shah and Perveen Akhtar for their constant support and enormous love which kept me motivated and happy while struggling for my studies and life here in Finland. I am also grateful to all of my brothers Kamran Fazal, Imran Fazal, Adnan Fazal and Irfan Fazal for their encouragement and moral support.

Finally to all my friends who made my stay in Tampere, Finland, so much enjoyable, happier and unforgettable and have always been with me in this so beautiful and memorable journey of my life. I would like to mention few of them here like Waqar Hussain, Fawad Mazhar, Matteo Maggioni, Andrea Milanti and Habib Ahmed. I am so grateful to all of you guys for being so nice and caring.

Tampere, April 2013

Rizwan Fazal

*To my Mom Perveen Akhtar and Dad Baghdad Hussain Shah, both
of whom made it possible for this work to be completed.*

love you Mom, Dad

CONTENTS

1. Introduction	1
1.1 Objectives and Scope of the Thesis	3
1.2 Organisation of the Thesis	3
2. WCDMA and OFDM Baseband Processing	4
2.1 WCDMA Baseband Processing	4
2.1.1 Spreading and Scrambling	6
2.1.2 Modulation	11
2.1.3 Rake Receiver Concept	11
2.2 OFDM Baseband Processing	18
2.2.1 IEEE 802.11a WLAN Overview	19
2.2.2 MAC Frame Structure for IEEE 802.11a	20
2.2.3 OFDM WLAN Baseband Algorithms	24
3. Platform Architecture	30
3.1 COFFEE RISC Core	30
3.1.1 Introduction to the Core	30
3.1.2 Registers and Timers	32
3.1.3 Operating Modes	33
3.1.4 Interrupts and Exceptions	34
3.1.5 Core Pipeline Structure	34
3.2 NineSilica MPSoC Platform	38
3.2.1 Introduction to the Platform	38
3.2.2 Network-on-Chip (NoC)	39
3.2.3 Computational Cluster	40
3.2.4 MPSoC Platform for SDR Applications	41
3.2.5 Communication and Synchronization	42
3.2.6 Hardware Implementation	43
4. Algorithms Mapping	44
4.1 WCDMA Parameters	44
4.2 WCDMA Baseband Processing	45
4.2.1 Multipath Estimation	45
4.2.2 WCDMA Demodulation	46
4.2.3 Channel Estimation	46
4.3 OFDM Parameters	47
4.4 OFDM Baseband Algorithms Mapping	48
4.4.1 OFDM Demodulation	49
4.4.2 Channel Estimation and Equalization	49
4.5 Symbols Demapping	50

5. Results	52
6. Conclusion	56
REFERENCES	58

LIST OF FIGURES

2.1	WCDMA basic frame structure [9, p. 81]	5
2.2	OVSF code tree [10, p. 83]	9
2.3	WCDMA downlink scheme [10, p. 103]	10
2.4	WCDMA uplink scheme [10, p. 109]	12
2.5	Digital baseband section of WCDMA receiver ©IEEE, 2007 [11]	13
2.6	Frame Structure for the downlink DPCH [9, p. 79]	18
2.7	OFDM baseband functional block diagram ©IEEE, 2007 [11]	19
2.8	PLCP Protocol Data Unit (PPDU) frame format ©IEEE, 1999 [17]	21
2.9	PLCP preamble ©IEEE, 1999 [17]	21
2.10	SIGNAL field bit assignment ©IEEE, 1999 [17]	23
2.11	Complete OFDM frame format ©IEEE, 1999 [17]	23
2.12	SERVICE field bit assignment ©IEEE, 1999 [17]	24
3.1	COFFEE core interface ©IEEE, 2003 [19]	32
3.2	Core pipeline stages [21]	35
3.3	NineSilica MPSoC platform ©IEEE, 2009 [18]	39
3.4	Single computational cluster ©IEEE, 2009 [18]	40
5.1	WCDMA baseband algorithms profiling results	53
5.2	OFDM baseband algorithms profiling results	54

LIST OF TABLES

2.1	Technical characteristics of WCDMA air interface [8, p. 27]	5
2.2	Rate-dependent parameters of 802.11a ©IEEE, 1999 [17]	20
3.1	Stratix II synthesis results of NineSilica MPSoC ©IEEE, 2009 [18] .	43
3.2	Stratix IV synthesis results of NineSilica MPSoC ©IEEE, 2010 [23] .	43
5.1	WCDMA baseband algorithms profiling results ©IEEE, 2013 [25] . .	52
5.2	OFDM WLAN baseband algorithms profiling results	54

ABSTRACT

TAMPERE UNIVERSITY OF TECHNOLOGY

Master's Degree Programme in Information Technology

Rizwan Fazal : Implementation of Communication Receivers as Multi-Processor Software

Master of Science Thesis, 60 pages

February 2013

Major: Digital and Computer Electronics

Examiners: Professor Jari Nurmi, Assistant Professor Tapani Ahonen

Department of Electronics and Communications Engineering, Tampere University of Technology

Keywords: Software Defined Radio, Multi-Processor System-on-Chip, Network-on-Chip

Over the years, we have seen changes in the mobile communication systems starting from Advanced Mobile Phone System (AMPS) to 3G Universal Mobile Telecommunications System (UMTS) and now to 4G Long Term Evolution (LTE) advanced. Also the mobile terminals have more features to offer comparatively when it comes to supported applications for example Wireless Local Area Network (WLAN), Global-Positioning System (GPS) and high speed multimedia applications. As the mobile terminals are now evolving towards multistandard systems, the traditional approach of designing radio platforms has now been replaced by more flexible and cost-effective solutions. The challenge imposed by this multistandard approach in the implementation of mobile terminals is to integrate several radio technologies into a single device. Sharing components and processing resources between different radio technologies is the key in the implementation of multistandard terminals. Software implementation of the components is preferred because of shorter lead-time of software development and it also costs less to carry out necessary redesigns with software. In an effort to take up this challenge, the designers proposed Software Defined Radio (SDR) that allows multiple protocols to work on a System-on-Chip (SoC). The SDR implementations can follow either the Multi-Processor System-on-Chip (MPSoC) or the Coarse-Grain Reconfigurable Array (CGRA) paradigm. For this thesis work, a

homogeneous MPSoC platform is used to accelerate the signal processing baseband algorithms of WCDMA and OFDM IEEE 802.11a WLAN standards. The performance comparison between single core and multi-core platforms has been made based on the number of clock cycles consumed. The idea is to exploit the inherent parallelism offered by homogeneous MPSoC platform and improve the execution times of computationally intensive algorithms like correlation operation and Fast Fourier Transform (FFT). The baseband signal processing components have been implemented in software and executed on a MPSoC platform to evaluate their performance. The multiprocessor platform has been used in an asymmetric manner in which each processing node has its own copy of application software and uses shared memory space for multiprocessor communication. Each of the processing nodes fetches and executes instructions from its own local instruction memory and are therefore independent from each other. Data Level Parallelism (DLP) has been exploited in the software implementation of the algorithms by performing identical operations simultaneously on different processors.

ABBREVIATIONS AND NOTATION

3G	Third Generation
3GPP	Third Generation Partnership Project
BTS	Base Transceiver Station
CGRA	Coarse Grain Reconfigurable Array
CPU	Central Processing Unit
DVFS	Dynamic Voltage and Frequency Scaling
FPU	Floating Point Unit
FFT	Fast Fourier Transform
FDD	Frequency-Division Duplexing
FDMA	Frequency-Division Multiple Access
GPS	Global Positioning System
IEEE	Institute of Electrical and Electronics Engineers
LTE	Long Term Evolution
MPSoC	Multi-Processor System-on-Chip
NoC	Network-on-Chip
OFDM	Orthogonal Frequency Division Multiplexing
PE	Processing Element
QPSK	Quadrature Phase Shift Keying
RF	Radio Frequency
RISC	Reduced Instruction Set Computing
SoC	System-on-Chip
SDR	Software Defined Radio
TDD	Time-Division Duplexing
TDMA	Time-Division Multiple Access
UE	User Equipment
UMTS	Universal Mobile Telecommunications System
WLAN	Wireless Local Area Network
WCDMA	Wideband Code Division Multiple Access

1. INTRODUCTION

Rapid evolution of communication standards in the last decade has put great challenges to both the platform hardware and software designers. Newly emerging wireless applications are quite demanding when it comes to computational power requirements considering the complexity of the algorithms being incorporated. It is also very challenging for an embedded platform to strictly satisfy the computational requirements where shortage of available resources and power is of significant concern. Applications like Global Positioning System (GPS) and Wireless Local Area Network (WLAN) for wireless internet access have become common requirements for the end user. The traditional approach of designing communication receivers is being replaced by more flexible solutions. Hardware components are being replaced by software solutions which are more flexible and cost-effective for future developments and this technology is termed as Software-Defined Radio (SDR)[1]. Regarding the SDR applications, different platform design paradigms have been in practice where some of them are broadly classified as Multi-processor System-on-Chip (MPSoC) and Coarse-Grain Reconfigurable Arrays (CGRA)[2][3].

MPSoC platform is a high performance platform used in different areas of applications including communications, multimedia and networking. Generally a MPSoC platform contains embedded processors, digital signal processors, digital logic and other mixed signal circuits[4]. Complex algorithms require large amount of computations and at the same time demand for strict constraints on performance, power and cost which at least can't be supported by simple hardware. The basic structure of a MPSoC is composed of several processing elements (PE) interconnected by an interconnection. The application context and requirements define the nature of PEs to be used and considered as a prime differentiating element between the two families of architectures termed as homogeneous and heterogeneous MPSoCs. In heteroge-

neous MPSoCs, the PEs used are of different types like general purpose processors, digital signal processors, hardware accelerators. On the other hand, homogeneous MPSoCs are composed of similar tiles instantiated several times. These PEs are interconnected by a Network-on-Chip (NoC) which is composed of Network Interfaces (NIs), routing nodes and links. To effectively manage the power, MPSoCs also incorporate distributed Dynamic Voltage and Frequency Scaling (DVFS)[5]. Heterogeneous MPSoCs are more power efficient and offer the best performance over power consumption trade-off while homogeneous MPSoCs are more flexible and scalable but less power efficient[6]. Homogeneous MPSoCs are also known as parallel architecture model where similar physical resources work simultaneously to divide the execution time and provide a speedup theoretically equivalent to the number of processing resources.

Considering the 3G and LTE wireless standards, WCDMA is used in 3G cellular networks and OFDM is used for LTE implementation. If we carefully analyze the baseband section which is responsible to recover the transmitted symbols, WCDMA uses correlation operation for demodulation while OFDM uses FFT operation. Both of these operations are computationally very intensive and demand high computational power from underlying hardware. However, both of these operations can be implemented in software and can be loaded on common platform like the one tailored for SDR applications[7]. Depending upon the platform, these intensive kernels may be running on dedicated accelerators where a single CPU is managing the overall system or evenly distributed among similar computational resources to improve the execution times. Hence programmability and reuse are the most important factors leading to higher design productivity. Design challenges lead to suitable design methodologies where the available options can be better analyzed for application deployment. Hence, baseband receiver algorithms can be implemented using higher level abstraction and can be ported to different platforms. On SDR tailored platform, these software defined functions can be loaded on user request and will provide the required services to the end user.

1.1 Objectives and Scope of the Thesis

Multiprocessor platforms are one of the favorite candidates for wireless applications and have proved themselves to be powerful computing engines. Heterogeneous and homogeneous MPSoC platforms offer best performances and both have their own pros and cons. The objective of this thesis work is to evaluate the performance of WCDMA and OFDM receivers bandband processing on a homogeneous MPSoC platform. The scope of the work is to implement the baseband signal processing algorithms of both the standards for a 32-bit Reduced Instruction Set Computing (RISC) processing core called COFFEE which has no Floating-Point Unit (FPU). The COFFEE RISC core is the main processing element which executes the software written in C language and compiled using `coffee-gcc` compiler. Later on, these baseband signal processing algorithms are implemented on a MPSoC platform which consists of nine similar Computational Clusters (CCs). Each of the CCs has single COFFEE core as a PE and contains data and code memories and a NI for inter-cluster communications using Network-on-Chip (NoC). Algorithms are implemented using fixed-point arithmetic and the results are compared with MATLAB simulation models. Once the algorithms are implemented and tested using single COFFEE core, these algorithms are then mapped on multi-processor architecture using parallel programming approach. The idea is to exploit the parallelism and distributing the workload among cores and compare the performance difference between single-core and multi-core architectures.

1.2 Organisation of the Thesis

The thesis is organized as follows; chapter 2 describes the technical background of WCDMA and OFDM WLAN 802.11a receiver baseband signal processing. The hardware platform architecture details are described in chapter 3 which includes 32-bit COFFEE RISC core and NineSilica MPSoC platform. Chapter 4 describes the implementation details of baseband algorithms for both the single-core and multi-core architectures. In chapter 5, the implementation results of algorithms mapping are explained in which the comparison between performance achieved is discussed followed by chapter 6 in which conclusions drawn are given.

2. WCDMA AND OFDM BASEBAND PROCESSING

In this chapter, the technical background of the WCDMA and OFDM baseband receiver is provided.

2.1 WCDMA Baseband Processing

Wide-band Code Division Multiple Access (WCDMA) is a third generation wireless interface standard being used in Universal Mobile Telecommunications System (UMTS) networks worldwide and managed by a group known as Third Generation Partnership Project (3GPP). The standard uses Frequency-Division Duplexing (FDD) and Time-Division Duplexing (TDD) schemes for multiplexing and supports data rates up to 2Mbps in its original format. This new standard gives the user more flexibility in terms of bandwidth (bandwidth on demand) and uses some special codes to spread the information over a wideband radio channel. It employs a 5MHz channel bandwidth and provides better performance and immunity to noise due to its higher signal bandwidth.[8, p. 25-26] Table 2.1 depicts the general technical characteristics of the WCDMA air interface standard. In the next paragraph, the fundamental concepts used frequently in WCDMA standard as well as how information is transferred from Base Transceiver Station (BTS) to User Equipment (UE) are explained.

In WCDMA system, the original information's bandwidth is changed to higher bandwidth by using the procedure of spreading. Each of the data symbols is modulated using higher rate signatures (codes) so that the resultant signal's bandwidth becomes equal to that of the code. The fundamental unit of measurement for these codes is called a chip and the number of chips modulated by each data symbol is referred

Table 2.1: Technical characteristics of WCDMA air interface [8, p. 27]

Channel bandwidth	5MHz
Frame length	10ms
Chip rate	3.84 Mcps
Duplex mode	FDD and TDD
Spreading factor	4-256 (uplink), 4-512 (downlink)
Data modulation	QPSK (downlink), BPSK (uplink)
Channel coding	Convolutional and turbo codes
Multirate	Variable spreading and Multicode
Downlink RF channel structure	Direct spread

to as the Spreading Factor (SF). A typical frame of the WCDMA standard has a duration of 10ms and is further subdivided into 15 slots as can be seen in Figure 2.1. The standard uses a fixed chip rate of 3.84Mcps (million chips per second) and hence one frame is composed of 38400 chips and each of the slots in a frame contains 2560 chips. The receiver receives this chip rate sequence from the RF-frontend and passes it to receiver's subsequent functional blocks for further processing and hence termed as chip rate processing (CRP). The spreading factors used are in the range from 4 to 256 which corresponds to symbol rates of 960 ksymbols/s and 15 ksymbols/s respectively. The modulation scheme used is Quadrature Phase Shift Keying (QPSK) which encodes two bits per symbol and the actual user data rate depends upon the selected slot format. In each slot, time-multiplexed information is available which includes pilot bits, physical layer signaling and user's data.

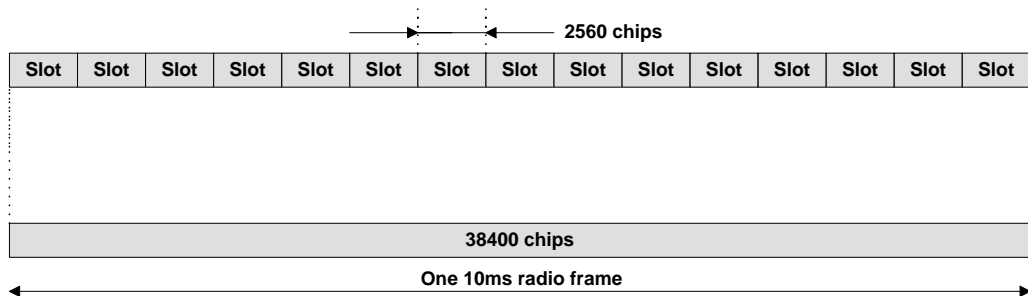


Figure 2.1: WCDMA basic frame structure [9, p. 81]

2.1.1 Spreading and Scrambling

In wireless communication systems, multiplexing techniques are used to improve the utilization of the available spectral density more effectively. Techniques like FDMA and TDMA have been in common use in cellular networks and are still used successfully in different applications to allow multiple users to access the network or resource simultaneously. To separate the users from each other, in FDMA system, each user is allocated a couple of channels (frequencies) for full duplex communication and in TDMA, different time slots are allocated to individual users to provide multiple accesses. The basic idea behind this multiple access technique is to facilitate as many users as possible but at the same time, maintaining the reliability and quality of service to individual users. In WCDMA system, special codes referred to as channelization (spreading) and scrambling codes are generally used for modulation. Before getting into the further details about these codes, there is a technique called spread spectrum which needs to be considered here to provide a background.

In spread spectrum technique, a low bandwidth signal (information) is turned into a high bandwidth signal which ultimately used to modulate a high frequency carrier signal for the transmission. There are a couple of schemes used in spread spectrum (SS) referred to as frequency hopping spread spectrum (FHSS) and direct sequence spread spectrum (DSSS). The bandwidth expansion is achieved by a coding process which is independent of the message signal being sent or the modulation scheme being used. The benefits behind SS are very significant that makes it a choice of interest among systems designers especially in applications where the privacy of information is of utmost importance and interception can be a catastrophe. In WCDMA, the spreading of information is achieved by multiplying user's data with quasi-random bits called chips derived from CDMA spreading codes. In the following sections, we will discuss about spreading and scrambling codes generation like where they come from and how they are used within the transmission path both for the uplink and the downlink.

In principle, channelization codes and scrambling codes have different uses when it

comes to different directions of the links. Channelization codes are usually small and exhibit the property of orthogonality which is very important for them but on the other hand, scrambling codes are quite long and are created from streams generally referred to as pseudo-random sequences. In FDD mode of the system, the channelization code is used to control data rate in the uplink direction while in the downlink direction it also separates the user. In the case of scrambling code, it separates the user in the uplink direction besides interference mitigation while in downlink direction; it helps in mitigating the interference. Both the user equipment (UE) and base station (Node B) uses the physical channels that are separated by channelization codes and sometimes defined in pair of codes with scrambling code.

Chip Rate

In WCDMA, chip is the fundamental unit of transmission and has a well-defined rate which is the reciprocal of chip duration that is 3.84 Mc/s (million chips per second). The chip rate is very important entity when we have to calculate the data rate which depends upon the spreading factor (SF) chosen. In principle, the spreading factor defines the number of chips used to spread a single bit of information or information symbol. At the transmitter end, each information symbol is exclusive OR'd with the channelization code which has a length corresponding to the spreading factor. Similarly, each of the information symbols in the data sequence are exclusive OR'd with the same spreading code and this is how the data rate gets increased and becomes equal to the chip rate. This is the information which is finally sent to the receiver and occupies wider bandwidth than that if it would have been sent without spreading. At the receiver end, considering an ideal communication channel which causes no interference to the data stream, the same chip sequence would be received. In order to recover the actual transmitted information symbols, the receiver will use the same spreading codes with the tight synchronization with the transmitter, and add (using X-OR gate) on a chip by chip basis the received sequence with the same spreading code sequence. By doing so, the receiver can successfully recover the transmitted information which is up-sampled.

Spreading Factor and Code Length

In the simplest terms, spreading factor defines the number of chips used to transmit a single bit of information and ultimately affects the data rate provided that the chip rate is kept constant which is 3.84 Mc/s. In WCDMA, different data rates can be achieved by changing the code length used to spread the data symbol starting from 4 to 512 chips. As stated above, if the chip rate is kept constant, then there is an inverse relation between the code length and the data rate. The advantage of this technique is that we are changing the data rate just by changing the code length (SF) and nothing else. Modulation technique also affects the data rate besides the channelization code being used and in the case of QPSK modulation, the data rate gets doubled. The data rate gets decreased if the length of the channelization code increased. The channelization code length increases by a multiple of 2 and consequently the data rate also decreased by the same factor. The code length can be computed by taking the ratio of the chip rate to the data rate.

Orthogonality and OVSF Code Tree

The channelization codes exhibit the property of orthogonality which makes them independent from each other and do not let them notice about a change made to any one of them. Mathematically, two codes expressed as 'Ci' and 'Cj' are orthogonal to each other if they are multiplied chip by chip and sum them over N chips of their lengths yield a result of zero. In a real scenario where multiple users are present in a cell, this property of orthogonality helps separating different users from each other and eliminating other users data from being recovered. Only the intended user can recover the information transmitted to him/her by using the same spreading code used at the source. Among the different types of orthogonal codes available like Walsh and Hadamard codes, the codes which have been chosen for WCDMA are orthogonal variable spreading factor (OVSF) codes. The OVSF codes have the same code sequences like Walsh and Hadamard except that there is a difference in how we index them. The spreading codes illustrated in Figure 2.2 range from SF 1 at the left side to SF 16 at the right side and can be created using a simple recursive algorithm. Starting from the left side, the initial code value is 0 with SF 1 (i.e.

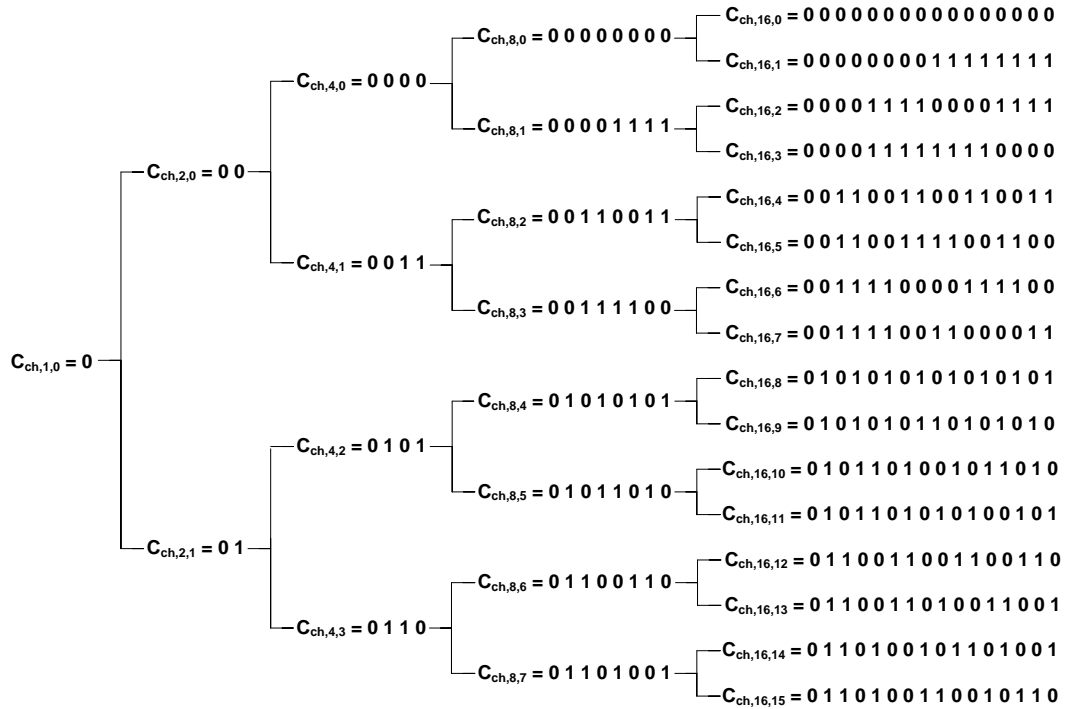


Figure 2.2: OVSF code tree [10, p. 83]

no spread) and splits into two branches where the upper branch repeats the same parent node sequence twice and so does the lower branch except that the second sequence is inverted. The algorithm proceeds in this fashion and subsequently builds four codes of length 4 and eight codes of length 8 and so on.

Before discussing about the baseband receiver implementation for the WCDMA protocol, it is necessary to recall the basic concepts that are most frequently used. So far we have concentrated mostly on the downlink part where channelization codes are used not only to separate the users but also to define the data rate for that user. However, in case of uplink, there is a different mechanism which is used to separate the users as the same OVSF codes can't be used for this purpose but only defines the data rate. In real world scenario, we have multiple cells operating simultaneously and may suffer from problems like inter-cell interference as the transmissions are asynchronous and the frequency bands are the same. In order to avoid unacceptable interference between the users, there is a need to introduce a second code in the

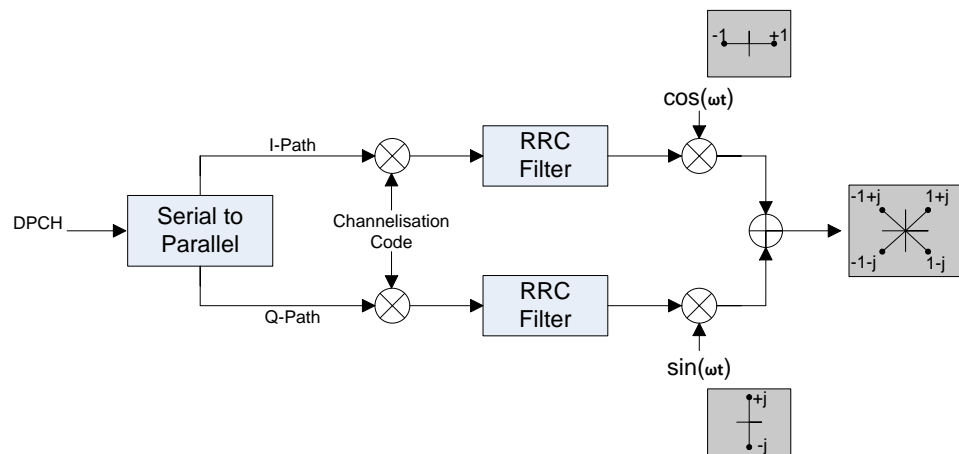


Figure 2.3: WCDMA downlink scheme [10, p. 103]

transmission path.

The scrambling code is a pseudo-random sequence of chips with amplitude $+1/-1$ and is applied at the chip rate to the spread data. So in this case, the information data is spread and then scrambled before transmission to the receiver, where it is descrambled by using the same scrambling code and despreading is performed to recover the actual transmitted information. Each user is assigned a unique scrambling code which ensures easy identification to specific UE in transmissions on the uplink and also rejects interference from other active UEs. Scrambling codes are pseudo-random sequences based on some algorithm that allows the creation of these in both the transmitter and the receiver and are commonly referred to as a pseudo-noise (PN) sequence. Scrambling codes need to have some properties like autocorrelation and cross correlation and in WCDMA system, ideal cross correlation is one that has a low value. A large auto correlation peak can be achieved for an ideal scrambling code if sequences are aligned and the other way around when they are not aligned. As far as cross correlation is concerned, an ideal performance would be to have very low cross correlation for all time offsets of the code and it is desired to keep this to a minimum as in practice it has a non-zero value.

2.1.2 Modulation

The WCDMA downlink consists of Dedicated Physical CHannel (DPCH) which is a stream of binary information. This binary information is converted into polar format as defined in 3GPP specifications according to which the binary '0' maps to a +1 polar signal and binary '1' maps to a -1 polar signal. After mapping, the DPCH passes through a serial to parallel (S/P) converter which alternately passes them to two streams termed as in-phase (I-plane) and quadrature plane (Q plane) symbols. Based on the required data rate, both of these polar streams are spread using the same channelization code. To remove the high frequency variations, data from both planes are passed through RRC filter followed by multiplication of I-plane data with a cosine function and Q-plane data with a sine function. The Figure 2.3 shows the WCDMA downlink transmission phase and constellation where I-plane takes the values of +1 and -1 and Q-plane takes the values of +j and -j represented using complex arithmetic. The composite signal will take the values of 45, 135, -45 and -135 degrees and corresponds to the vector sum of I and Q. [10, p. 102-103]

In WCDMA uplink transmissions, there is a difference in the type of information the I-plane and Q-plane carry as shown in Figure 2.4. I-plane carries DPDCH channel which consists of user traffic and control signaling and the spreading factor used for it varies between 4 and 256 which corresponds to data rates between 960 kb/s and 15 kb/s. On the other hand, the Q-plane carries DPCCH which carries pilot bits, power control (TPC) bits, feedback mode indicator (FBI) bits and transport format combination indicator (TFCI) bits. The DPCCH uses a spreading factor of 256 which corresponds to physical channel data rate of 15 kb/s and uses the channelization code of 0. The modulation used for uplink is similar to that used for downlink and hence uses the same I and Q planes which are filtered using RRC filter and then quadrature up-conversion procedure is applied. [10, p. 108-110]

2.1.3 Rake Receiver Concept

The rake receiver is considered as an efficient implementation of a receiver used in WCDMA based systems to recover the transmitted symbols. There are independent

physical channels used to transport data, control and pilot information which are usually time-multiplexed in these physical channels. It is the responsibility of the receiver to de-multiplex the data and control information. The recovered data symbols are forwarded to bit rate processing block for error detection and correction that may have occurred during transmission while the control information is correctly acted upon. The process of recovering the transmitted symbols is accomplished by the rake receiver which has to execute different signal processing algorithms. The baseband functional blocks in this receiver includes multipath searcher, rake fingers, channel estimator and the maximal ratio combiner. By using these baseband blocks, rake receiver performs the operation of synchronization, demodulation, channel estimation and channel equalization. A high level block diagram of a rake receiver is shown in Fig 2.5. In the following subsections, we will discuss in sufficient length about the baseband functions performed by these individual blocks of the rake receiver.

Timing Synchronization

When the user switches on the mobile terminal, the terminal starts searching for the closest base station or cell so that the services provided by the core network can be used. The user equipment searches for the nearby cell and gets the timing information which includes slot timing, frame timing and the cell ID (identification). The operation performed to get all this information is called the cell search procedure

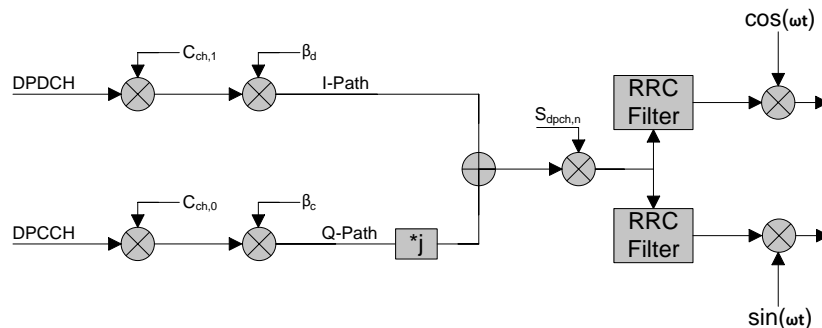


Figure 2.4: WCDMA uplink scheme [10, p. 109]

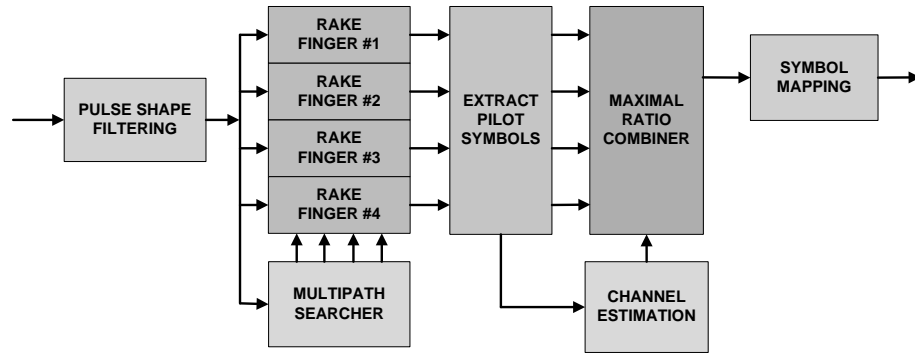


Figure 2.5: Digital baseband section of WCDMA receiver ©IEEE, 2007 [11]

and is described in the next subsection.

Cell Search

The cell search is the algorithm performed by the user equipment to detect the presence of cells it has no information about. The user equipment follows a three-stage procedure to find and then synchronize to a cell and is based on three fundamental physical layer channels. These signaling channels are available in every cell and referred to as Primary Synchronization Channel (P-SCH), Secondary Synchronization Channel (S-SCH) and Primary Common Pilot Channel (P-CPICH). The three stages of the cell search operation are slot synchronization, frame synchronization and scrambling code identification.

The objective of the slot synchronization stage is to detect the presence of cell and to find the slot start time. For this purpose, P-SCH is used in which a known 256-chip-long sequence is broadcasted at the beginning of every slot on downlink. The receiver correlates the received signal with the locally stored P-SCH code sequences to identify its presence. The series of pulses are found at the output of matched filter at the start of each slot and hence provides an indication of the slot boundaries. In frame synchronization, the receiver uses the S-SCH channel to determine the frame synchronization and scrambling code. The S-SCH uses 256-chip-long codeword for each slot and at the start of each slot, a different codeword is transmitted. The order and the definition of these code words are very important as this is how the

UE identifies the code sequence to find the frame timing and code group. In the third stage, the identified code group is used to find the exact primary scrambling code used by the cell. The received signal is correlated with the eight different scrambling codes which belong to the identified code group. The code resulting in strongest correlation output is selected as the cell's primary scrambling code.

Multipath Propagation

In radio propagations, the signal transmitted from an antenna may suffer from reflections and diffractions due to obstacles like buildings in the coverage area. The signal travels through multiple independent paths and hence at UE or Node B, it arrives along with multiple reflections. These multiple signals are called multipath components and this phenomenon is generally referred to as multipath propagation. The impact of these multipath components can be ignored in systems with small bandwidth but the effects on system performance needs to be considered if the bandwidth is higher. In narrow band communication system, an optimum receiver uses correlation and integration methods and operates efficiently in flat Rayleigh fading situations. A single correlator can provide optimum performance in narrow band systems but in multipath fading channel, it suffers from problems. In multipath propagation, additional correlators are used to overcome the inter-symbol interference which can degrade performance and hence leads to a design of a complete rake receiver.

In a typical spread spectrum receiver, a locally generated de-spreading waveform is multiplied with the received signal on a sample by sample basis. The resulting signal is then integrated over a period of transmitted symbol and finally the output is sampled. In multipath propagations, the despreading and descrambling sequence is time-aligned with the received multipath component which corresponds to specific path and hence the time delay. The despreading signal has to be time-aligned with one of the multipath components to despread it correctly. The signal arrival time must be known and hence synchronized with the despreading and descrambling waveform. Depending upon the number of correlators used, the timing arrangements

need to be made for the strongest multipath components. The outputs of the correlators are then combined which leads to a better signal to noise ratio (SNR) than the SNR of individual multipath components. To obtain net power gain, the signals are added coherently and the noise is added non-coherently. The time difference between the correlators ensures that we can add together the outputs and combine them correctly.

Multipath Estimation

In multipath radio propagations, the User Equipment (UE) receives multiple copies of the single transmitted pulse. These multiple components may affect the receiver performance if not properly taken into account. Due to signal's high bandwidth, the effect of multipath components cannot be ignored. Hence in WCDMA systems, multiple rake fingers are used where each finger corresponds to a specific multipath component according to its delay profile. The multipath searcher identifies the strongest signal components and allocate each of them with a rake finger. Depending upon the environment, the signal components travel through different paths and arrive at different time instants to UE. In [10, p. 189], the reported highest path delays can be $5\mu\text{s}$ in an urban environment and $20\mu\text{s}$ in hilly areas. To obtain multipath diversity, the time difference of multipath components should be at least $0.26\mu\text{s}$ which is the duration of a single chip [8, p. 31]. In this case, the WCDMA receiver can separate those multipath components and combine them coherently. A known pilot sequence is matched with the received signal to perform multipath estimation operation as shown in Eq. 2.1

$$y(k) = \sum_{l=0}^{L-1} t^*(l)r(k+l) \quad (2.1)$$

where $y(k)$ is the output of the matched filter, $t^*(l)$ is the complex conjugate of pilot symbol and L is the length of the correlation [11]. The multipath estimation process has been described as a two-stage process namely as acquisition and tracking in [12]. In acquisition stage, the arrival of first signal component is detected and in tracking stage, the changes in multipath taps are followed within a certain time span. The amplitude of the correlation peak corresponds to the gain of the multipath

component and a path delay can be measured by using the time offset relative to the first peak arrival. The noise and interference caused from other users may affect the system performance, hence the process of averaging the sequential estimation windows non-coherently is used and is shown in Eq. 2.2

$$y_{ave}(k) = \frac{1}{M} \sum_{m=0}^{M-1} |y_m(k)|^2 \quad (2.2)$$

where $y_m(k)$ is the k th element of the m th correlation window [11]. In [13], it is stated that the multipath searcher receives the pseudo-noise (PN) sequence from Base Transceiver Station (BTS) as a result of cell search operation. The alignment of this PN sequence corresponds to the strongest multipath and is used to find other multipaths by correlating it with the P-CPICH symbols. The rake fingers are then configured accordingly based on the relative offset of the multipath. The multipath searcher operates continuously as it is highly likely that the UE changes its position frequently.

Demodulation

In a narrow band receiver, a single correlator is generally used to recover the transmitted symbols. A correlator multiplies the received signal with a copy of the transmitted pulse and integrates the output after the multiplication process for the duration of the symbol period. Once this operation completes, the integrator is reset and decision can be made on the transmitted symbol. All this is quite optimum when it comes to narrow band transmissions but it may suffer from problems when bandwidth is higher due to multipath fading channel. In WCDMA systems, the receiver has more than one correlator and is assigned to one of the multipath components. The output of the i^{th} rake finger is shown in Eq. 2.3

$$\hat{d}_i(n) = \sum_{l=0}^{L_{sf}-1} c_s^*(l + nL_{sf})r(l + \hat{\tau}_i + nL_{sf}) \quad (2.3)$$

where c_s represents the combined spreading and scrambling codes, L_{sf} is the spreading factor and $\hat{\tau}_i$ is the multipath estimate for the i th rake finger [11]. The correlators perform despreading and descrambling operations and finally the outputs are com-

bined. As a consequence, a large bandwidth signal with low power spectral density turns into a narrow-band signal with a higher power spectral density. The benefit of combining signals this way is the improved Signal-to-Noise Ratio (SNR) of the resultant signal comparatively with the SNRs of individual components [10, p. 197]. The multipath components have some impact on the output of individual fingers but it can be minimized by using a large spreading factor.

Channel Estimation

To add the rake fingers output coherently and synchronously, the channel's phase and amplitude must be estimated for each of the identified paths. The methods generally used for this process includes data aided channel estimation, decision-directed channel estimation and blind-channel estimation. Channel estimates can be obtained either by using one or any combination of the above mentioned procedures. The sources available to perform this operation include Common Pilot CHannel (CPICH) and the pilot symbols time-multiplexed within the slots of Dedicated Physical Control CHannel (DPCCH) [14]. The DPCCH is transmitted together with the DPDCH within each slot of the DPCH frame and consists of control information bits like TFCI bits, the power control bits and of course the pilot bits. The slot format of the downlink DPCH is shown in Fig 2.6. The symbols extracted in demodulation operation performed in rake fingers can be expressed as

$$\hat{d}_i(n) = \alpha_i d(n) + w(n) \quad (2.4)$$

In Eq. 2.4, $d(n)$ is the transmitted symbol, α_i is complex attenuation of the i^{th} multipath, $\hat{d}_i(n)$ is the output of the rake finger and $w(n)$ is additive noise [11]. The channel estimate of the i^{th} multipath can be computed when the transmitted symbol is known and is expressed as

$$\hat{\alpha}_i \simeq \frac{\hat{d}_i(n)}{d(n)} \quad (2.5)$$

Based on the chosen slot format, time-multiplexed pilot symbols of DPCCH are demultiplexed from the received symbols and then correlated with the known pilot

symbol sequence. For improved performance, preliminary channel estimates are used to make symbol decisions and then these symbols are used as pilot symbols for the next stage to get more accurate estimates. As far as CPICH is concerned, there is at least one such channel available in every cell and uses a fixed primary scrambling code, hence named as Primary Common Pilot Channel (P-CPICH). It uses the spreading factor of 256 and does not carry any higher layer information. [8, p. 103]

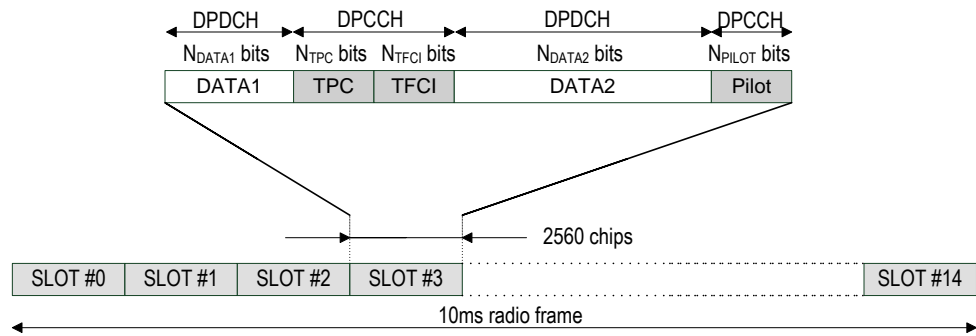


Figure 2.6: Frame Structure for the downlink DPCH [9, p. 79]

2.2 OFDM Baseband Processing

Orthogonal Frequency Division Multiplexing (OFDM) is considered as a promising solution for wired and wireless communication standards to achieve higher data rates and immunity to issues like multipath fading and inter-symbol interference (ISI). Instead of a single carrier system, OFDM uses multi-carrier modulation (MCM) scheme in which multiple carrier frequencies are used to modulate parallel data streams and hence transmitting the data in parallel over the communication channel. These carrier frequencies are orthogonal to each other and contain low rate data due to lower bandwidth of individual channels. Digital audio broadcast (DAB), digital video broadcast (DVB), asymmetrical digital subscriber line (ADSL) Discrete Multi-Tone (DMT), wireless LAN standards and now the LTE mobile communications are the popular applications area of this tremendous technology [15]. A high-level block diagram of OFDM baseband receiver is shown in Fig. 2.7.

An OFDM receiver basically performs the reverse operations of the transmitter. In

the beginning, it estimates the frequency offset and symbol timing by using the special training symbols in the preamble. FFT operation is then performed to every OFDM symbol to recover the 52-QPSK values of all subcarriers. The reference phase and amplitude of the constellation on each subcarrier is required to estimate the bits at receiver end. Correction for the channel response as well as remaining phase drift can be made using the training symbols and pilot subcarriers. The recovered symbols can then be demapped into binary values after which a Viterbi decoder can decode the information bits. Every OFDM packet contains a preamble which is essential to perform start-of-packet detection, automatic gain control, symbol timing, frequency estimation and channel estimation. A guard interval is inserted at the end of each OFDM symbol to eliminate the intersymbol interference almost completely. Also the guard interval is chosen larger than the expected delay spread such that the multipath components from one symbol cannot interfere with the symbol that follow.

2.2.1 IEEE 802.11a WLAN Overview

IEEE 802.11a is one of the approved WLAN standards which uses OFDM system and hence transmits and receives information using several sub-carriers simultaneously. Inverse Fast Fourier Transform (IFFT) and Fast Fourier Transform (FFT) are used for transmitting and receiving those sub-carriers respectively. The standard uses a 5 GHz Unlicensed National Information Infrastructure (U-NII) band and has the capability of transmitting at the maximum data rate of 54Mbps. In 802.11a

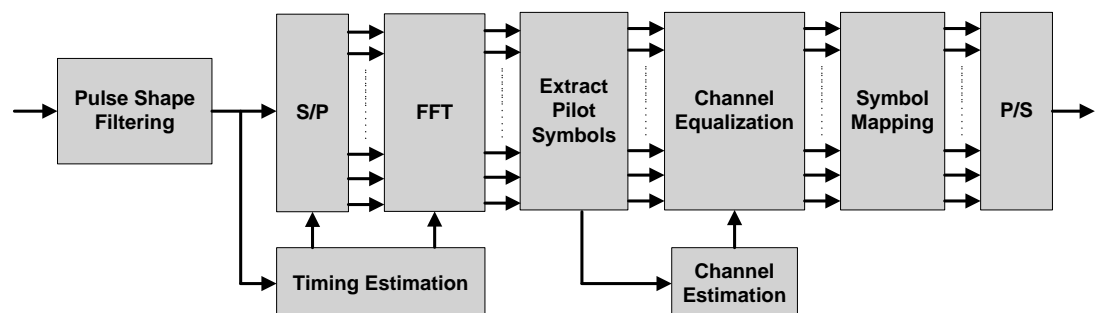


Figure 2.7: OFDM baseband functional block diagram ©IEEE, 2007 [11]

standard, the other supported data rates are 6, 9, 12, 18, 24, 36, and 48 Mbps and it is mandatory to transmit/receive at 6, 12 and 24 Mbps. The system has a bandwidth of 20MHz which splits into 64 carrier frequencies resulting in a sub-carrier frequency spacing of 0.3125 MHz. From these 64 sub-carriers, 48 sub-carriers are used to transmit the user data and 4 of them are used for pilot reference signals whereas the remaining 12 subcarriers are not used. The modulation schemes used are Binary Phase Shift Keying (BPSK), Quadrature Phase Shift Keying (QPSK), 16 Quadrature Amplitude Modulation (QAM) and 64 QAM. Channel coding can be incorporated to achieve the same data rate but with improved BER performance. In wireless systems, Convolutional codes have been the most widely used channel codes for the last decades.[16, p. 36-38] Table 2.2 describes the physical layer specifications of the IEEE 802.11a WLAN standard.

Table 2.2: Rate-dependent parameters of 802.11a ©IEEE, 1999 [17]

Data rate (Mbps)	Modulation	Coding rate (R)	Coded bits per subcarrier (N_{BPSC})	Coded bits per OFDM symbol (N_{CBPS})	Data bits per OFDM symbol (N_{DBPS})
6	BPSK	1/2	1	48	24
9	BPSK	3/4	1	48	36
12	QPSK	1/2	2	96	48
18	QPSK	3/4	2	96	72
24	16-QAM	1/2	4	192	96
36	16-QAM	3/4	4	192	144
48	64-QAM	2/3	6	288	192
54	64-QAM	3/4	6	288	216

2.2.2 MAC Frame Structure for IEEE 802.11a

The IEEE 802.11a standard uses a Carrier Sense Multiple Access with Collision Avoidance (CSMA/CA) protocol for its Medium Access Control (MAC) layer and uses Clear Channel Assessment (CCA) scheme to check the availability of the medium. Also the sender expects an acknowledgement from the receiver as collisions or fading may occur which may corrupt the data. Physical Layer Convergence

Protocol (PLCP) and Physical Medium Dependent (PMD) are the two sub-layers of the 802.11a PHY layer where PLCP interacts with the MAC for the exchange of information. Figure 2.8 shows the complete frame format of the IEEE 802.11a WLAN standard.

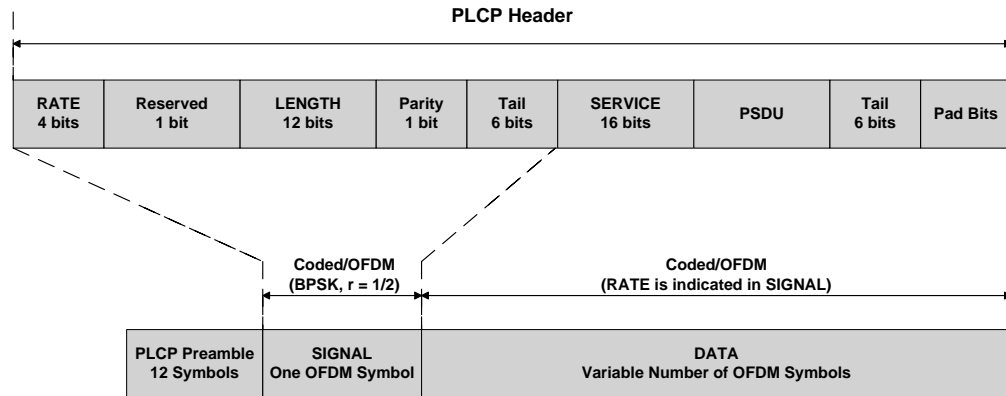


Figure 2.8: PLCP Protocol Data Unit (PPDU) frame format ©IEEE, 1999 [17]

The PPDU frame consists of PLCP preamble, header and the data field. The PLCP preamble consists of 10 short training symbols and 2 long training symbols as shown in Figure 2.9 and used for packet detection and symbol timing information.

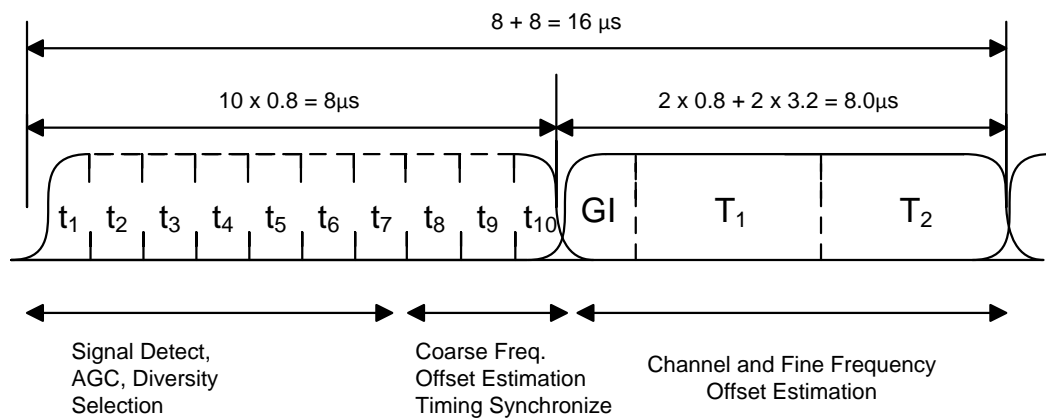


Figure 2.9: PLCP preamble ©IEEE, 1999 [17]

In Figure 2.9, the ten short training symbols are from t1 to t10 and the two long training symbols are T1 and T2. Both the short and long training symbol sequences are of $8\mu\text{s}$ duration with the total time of $16\mu\text{s}$. The sequence S shown in eq. 2.6 is used to modulate the 12 subcarriers out of 52 by each of the short training symbols.

$$\begin{aligned}
S_{-26,26} = & \sqrt{(13/6)} \times \{0, 0, 1 + j, 0, 0, 0, -1 - j, 0, 0, 0, 1 + j, 0, 0, 0, -1 - j, 0, 0, 0, \\
& -1 - j, 0, 0, 0, 1 + j, 0, 0, 0, 0, 0, 0, 0, -1 - j, 0, 0, 0, -1 - j, 0, 0, 0, 1 + j, \\
& 0, 0, 0, 1 + j, 0, 0, 0, 1 + j, 0, 0, 0, 1 + j, 0, 0\} \tag{2.6}
\end{aligned}$$

There is another sequence L which modulates 53 subcarriers for each of the long training symbols and is shown in eq. 2.7. There is a Guard Interval (GI) between the short and long training symbols to avoid inter-symbol interference. The duration of this guard interval is $1.6\mu s$

$$\begin{aligned}
L_{-26,26} = & \{1, 1, -1, -1, 1, 1, -1, 1, -1, 1, 1, 1, 1, 1, 1, -1, -1, 1, 1, -1, 1, -1, 1, 1, 1, 1, \\
& 0, 1, -1, -1, 1, 1, -1, 1, -1, 1, -1, -1, -1, -1, -1, 1, 1, -1, -1, 1, -1, 1, -1, \\
& 1, 1, 1, 1\} \tag{2.7}
\end{aligned}$$

Hence, these short and long repetitions of known sequences are collectively termed as preamble which is used for synchronization purpose. After the preamble part, there is another field called SIGNAL field which is encoded using BPSK modulation of the subcarriers. There is only one symbol in this SIGNAL field which consists of 24 bits which are not scrambled. The type of information conveyed by this field includes the RATE and the LENGTH of the TXVECTOR as shown in Figure 2.10. The first four bits are reserved for RATE which represents the type of modulation and the coding rate which is convolutional coding at $R = 1/2$. The bits from 5-16 represent the LENGTH field and bit 4 is reserved for future use. The supported data rates mentioned in section 2.2.1 can be selected by using the specific bit patterns already assigned for them in the standard. The LENGTH field is an unsigned 12-bit integer and indicates the number of octets in the PSDU need to be transferred as requested by the MAC layer. There is a parity bit P which is a positive (even) parity for the bits 0-16. The last field is called the TAIL field which is 6 bits long and all of them are set to zero as can be seen in figure 2.10. After the SIGNAL field, the

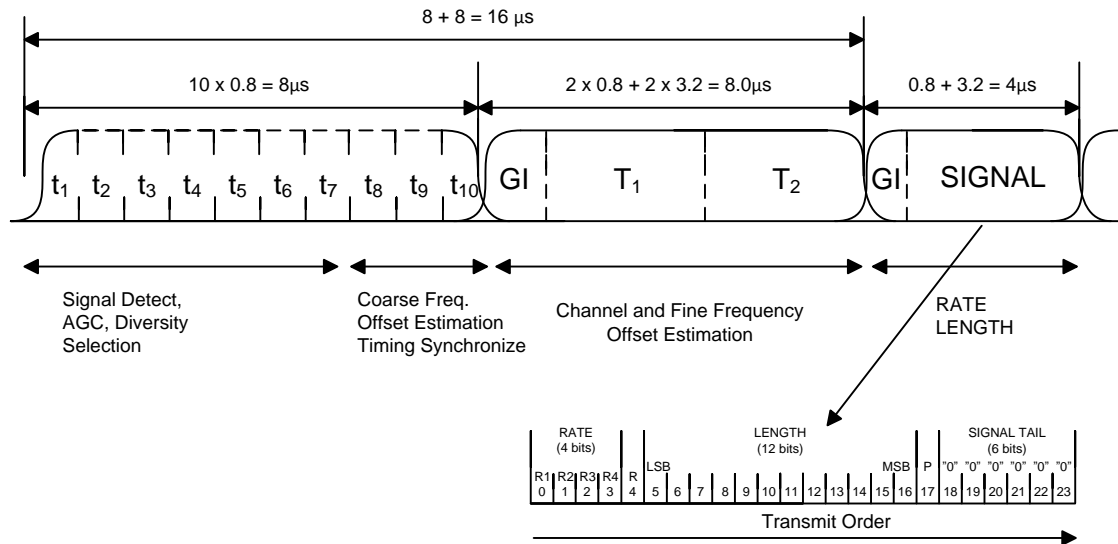


Figure 2.10: SIGNAL field bit assignment ©IEEE, 1999 [17]

DATA field starts as shown in figure 2.11.

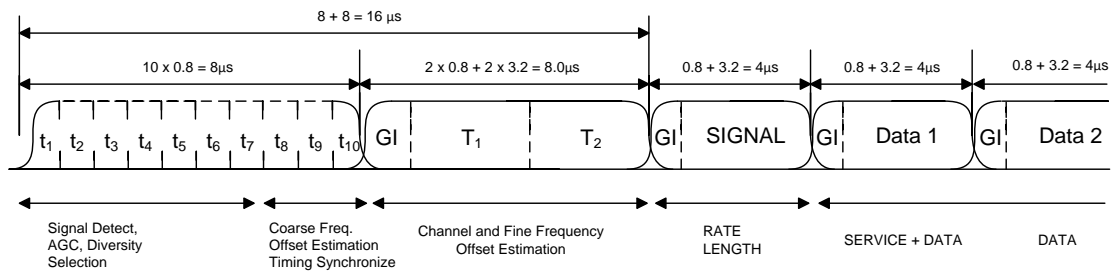


Figure 2.11: Complete OFDM frame format ©IEEE, 1999 [17]

The data bits are all scrambled and this DATA field contains the SERVICE field, the PSDU, the TAIL bits and the PAD bits. The SERVICE field consists of 16 bits where the bits 0-6 are used to synchronize the descrambler in the receiver and the bits from 7-15 are all reserved for future use as shown in figure 2.12.

The scrambler initialization bits as well as the remaining 9 reserved bits are all set to zero. To return the convolutional encoder to the 'zero state', the 6 bits of the tail field are set to zero. Finally the pad bits in the frame are used to keep the number of data bits a multiple of N_{CBPS} that is the number of coded bits per OFDM symbol (48, 96, 192 or 288). Hence the length of the message is multiple of N_{DBPS} that is the number of data bits per OFDM symbol. Also the appended bits are set to zero

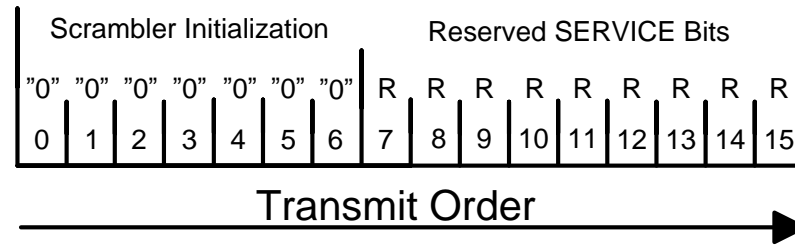


Figure 2.12: SERVICE field bit assignment ©IEEE, 1999 [17]

and are scrambled by using the remaining bits in the DATA field.

2.2.3 OFDM WLAN Baseband Algorithms

The digital baseband section of OFDM WLAN receiver executes baseband algorithms so that the transmitted symbols can be extracted. The baseband section generally performs synchronization, demodulation, channel estimation and equalization operations. The following subsections will explain these operations in sufficient length pertaining to OFDM WLAN receiver.

Time and Frequency Offset Estimation

In order to extract the transmitted data symbols accurately, the receiver has to synchronize itself with the incoming packet so that it can perform desired operations on the correct set of samples which is generally referring to the same OFDM symbol. The synchronization process includes packet detection and symbol timing information which can be obtained using the packet's preamble part. The preamble is composed of ten repeated short symbols and two repeated long symbols where each short symbol consists of 16 samples and each long symbol consists of 64 samples. There is a guard interval between the short training symbols and long training symbols and contains 32 samples taken from the end of LTS. According to the IEEE 802.11a standard, the first seven short symbols would be used for packet detection, automatic gain control (AGC) and diversity selection for Multiple Input and Multiple Output (MIMO) systems [17]. The remaining three short symbols should be used for Coarse Frequency Offset (CFO) calculation and time synchronization. Channel

Estimation and Fine Frequency Offset (FFO) calculation can be made using LTS and can also be used to refine the time synchronization estimates. Hence in every new transmission, the transmitter adds this preamble and then appends the actual data symbols.

It is critical for a typical wireless receiver to detect the presence of a packet transmission in a wireless channel where various complicating factors distort the signal properties. Regarding OFDM modulation, the orthogonality among subcarriers may get affected due to offset between transmitter and receiver subcarrier frequencies which may cause significant degradation in system performance. Therefore to maintain the orthogonality among subcarrier frequencies, the transmitter and receiver must be precisely synchronized and this requires accurate frequency offset calculation at the receiver. But the first task is to detect the presence of a packet by exploiting the repeated pilot symbols and to estimate the start of the Fast Fourier Transform (FFT) window. We can get reliable and accurate estimates using preamble based synchronization scheme and this operation gets completed in about first one to two starting symbols.

Packet Detection

In 802.11a WLAN standard, the short training symbols can be used for packet detection as they are identical and repeated for 10 times in the beginning of every data packet. The packet detection can be achieved using delay and correlate method in which a received signal is correlated against a delayed version of itself. The delay and correlate method will yield an output $y(k)$ which is given by

$$y(k) = \sum_{l=0}^{L-1} r(k+l)r^*(k+D+l) \quad (2.8)$$

Here $r(k)$ is representing the signal received, $()^*$ identifies the complex conjugate operation, distance between two consecutive symbols is represented by D and L is the length of the correlation. The received signal power during the correlation period can be used to normalize the correlation output $y(k)$ as given by

$$p(k) = \frac{1}{2} \sum_{l=0}^{L-1} |r(k+l)|^2 + |r(k+D+l)|^2 \quad (2.9)$$

Here $p(k)$ is representing the energy of the received signal which can be used to compute the decision metric as given by

$$M(k) = \frac{|y(k)|^2}{(p(k))^2} \quad (2.10)$$

The decision metric $M(k)$ reaches its maximum value when two different correlation windows match exactly. The first crossing-point of this metric against a preset threshold value gives indication of packet presence. Hence, the value of $M(k)$ is compared against a threshold value and detection can be observed if correlation peak crosses it.[11]

Symbol Timing Estimation

The symbol timing information is needed to identify the symbol boundaries so that the FFT operation can be performed on the correct set of samples. Once the packet is detected, the receiver starts searching for symbol boundaries using the same delay and correlate algorithm. In 802.11a standard, the receiver uses the long training sequence for symbol timing estimation by exploiting the sequential repeated known symbols. Matched filter approach can also be applied as an alternative and the output is then computed as

$$y(k) = \sum_{l=0}^{L-1} t^*(l)r(k+l) \quad (2.11)$$

Here $t(l)$ is representing the training symbol and the symbol timing estimate would correspond to the index giving the maximum value of $y(k)$ within an observation window.

$$\hat{\tau} = \arg \max_k \{|y(k)|^2\} \quad (2.12)$$

The received signal is correlated against the long training sequence and the edge of the first FFT window is computed by detecting the largest correlation peak. The

packet detection is taken into consideration as a beginning of the search window whose length is determined by longest expected propagation delay.[11]

Frequency Offset Estimation

A phase difference is introduced as a consequence of frequency offset between transmitter and receiver subcarrier frequencies that may lead to intersymbol interference. This offset can be estimated by observing the phase difference between the two identical symbols which is also proportional to the separation between the two transmissions. In 802.11a standard, the short training symbols can be used for this purpose by using the same delay and correlate method. The frequency offset estimate can be expressed as

$$\hat{f}_o = -\frac{1}{2\pi DT_s} \angle y(\hat{\tau}) \quad (2.13)$$

Here T_s is representing the sampling period and D is distance between two training symbols measured in samples. $y(\hat{\tau})$ is the correlation output at index $\hat{\tau}$ which gives its maximum value of $y(k)$ within the observation window.[11]

Demodulation

Once the receiver has packet and symbol timing information, the next step is to recover the transmitted data bits. The WLAN OFDM demodulator performs 64-point FFT operation to recover the transmitted subcarriers and hence makes decision on transmitted bits. Depending upon the type of constellation used, the received symbols are estimated using the maximum-likelihood decision followed by hard or soft decisions to obtain the assigned bits to those estimated symbols. The advantage of using FFT is the reduced number of multiply-accumulate operations rather using DFT implementation using correlation. By using the DFT operation, the n th symbol output of the i th subcarrier will be determined as

$$\widehat{D}_i(n) = \sum_{m=0}^{M-1} r(m + \hat{\tau} + n(L_{fft} + L_{cp})) W_M^{mi}, \quad i = 0, \dots, M-1 \quad (2.14)$$

Here M is representing the length of the transform, $\hat{\tau}$ is symbol timing estimate, length of the FFT window is represented by L_{fft} , L_{cp} is the length of the cyclic prefix and $W_M = e^{-j2\pi/M}$. [11]

Channel Estimation

In WLAN OFDM systems, the training data transmitted on every subcarrier is used to perform the channel estimation operation. The long training symbols in the WLAN preamble are used to estimate the channel response. The quality of the channel estimate can be improved by averaging the contents of two long training symbols as they are identical. In WLAN systems, the channel conditions generally do not change during a data packet and hence assumed to be a quasistationary channel. Thus channel estimation in OFDM is made using pilot symbols available in the preamble of a data packet and valid for the entire packet. Considering a non-frequency selective channel, after demodulation the received k^{th} symbol is denoted as

$$y(k) = h(k)x(k) + n(k) \quad (2.15)$$

Here $h(k)$ is representing the complex channel coefficient corresponding to the k^{th} symbol and $n(k)$ is additive white gaussian noise. As the transmitted symbols are known, the channel estimate can be computed as

$$\hat{h}(k) \approx \frac{y(k)}{x(k)} \quad (2.16)$$

The channel estimates can be computed using Eq. 2.10 for all the subcarriers using the training symbols employed in the preamble of the packet. The effect of noise can be mitigated by averaging the several identical transmitted symbols in the preamble. [12]

Symbols Demapping

Having performed the operations of synchronization, demodulation and channel estimation, finally it is time for the receiver to make decisions on the transmitted

symbols. Depending upon the type of modulation used, the decision boundaries determine how received symbols are mapped to bits. Considering the case of QPSK modulation, there are four constellation points which are 90 degrees apart from each other on a constellation diagram with I and Q axes. The maximum-likelihood decision is the constellation point that is closest to the received symbol. The computed raw data symbols need to be corrected by using the maximum-likelihood approach to determine the actual constellation points. In both the WCDMA and OFDM baseband receiver implementations, the transmitted data symbols will be determined using the technique of maximum-likelihood in which a relative distance between received symbols and one of the constellation points is calculated and compared.

3. PLATFORM ARCHITECTURE

The hardware platform used in this experimental work is a homogeneous Multiprocessor System-on-Chip (MPSoC) platform called NineSilica. The platform consists of 9 Computational Clusters (CC) which are interconnected through a hierarchical Network-on-Chip (NoC). Each of the CCs contains a 32-bit general purpose Reduced Instruction Set Computing (RISC) processing core called COFFEE as a main processing element (PE), data and code memories and an NI.[18] The complete platform has been designed and developed in the Department of Electronics and Communications Engineering, Tampere University of Technology. The following subsections will explain the architecture of COFFEE RISC core, the CC and the MPSoC platform in sufficient detail.

3.1 COFFEE RISC Core

In this section, an introduction to the core is provided and also the hardware peripherals available for application development purpose are described. The core execution pipeline is also described in this section.

3.1.1 Introduction to the Core

COFFEE is an open source RISC processor core also known as load and store machine which has been designed and developed in Tampere University of Technology. The hardware features of the processing core are as follows;

- Harvard architecture
- 6 pipeline stages
- Multiplication of 16-bit and 32-bit operands
- Full precision 64-bit multiplication result in 4 clock cycles

- Two Separate register banks for fast context switching
- SW-configurable through a memory-mapped register bank
- Super user mode for OS-like functionality
- Memory protection mechanism
- Built-in 12-input interrupt controller
- Two timers
- Coprocessor interface

Some of the common features of the core like registers, timers, operating modes and interrupts/exceptions will be described in more detail in the sections that follow. Figure 3.1 shows an interface diagram of the COFFEE processor. Supporting separate interfaces for data and instruction memories offer freedom to choose any of the memory type as long as interface timing requirements are met. Large and slow main memories can be interfaced directly because of multi-cycle access support and number of cycles per access can also be configured. Sharing of data bus might also be considered for simple systems having single system bus and no cache memory. Up to four coprocessors can be connected to COFFEE RISC core whose interface is much like memory interface. Dedicated instructions are provided to move data and instructions to and from coprocessors. Coprocessor ID (identification) is specified using 2 bits and a field of 5 bits to specify the register index constitutes a total of 7 bits addressing. An interrupt signal is also provided in the interface such that the coprocessor can interrupt the core in case of an exception. Also the coprocessor can be connected to different clock domains which is considered as an important feature of the coprocessor interface.[19]

Referring to the interface diagram of the COFFEE core shown in Figure 3.1, PCB (Peripheral Control Block) is provided to communicate with peripheral devices around the core. PCB_WR and PCB_RD signals can be asserted using the memory space reserved for peripherals and hence directing the access to the PCB. COFFEE

core reads its boot address from data bus if the signal `BOOT_SEL` is high and selects the address of the first executed instruction. The COFFEE core can be put in power saving mode if the system is battery powered by enabling this feature using the `STALL` signal. Software execution resumes as soon as the `STALL` signal is released as the clock to the core is not disabled but data in registers got frozen.[19]

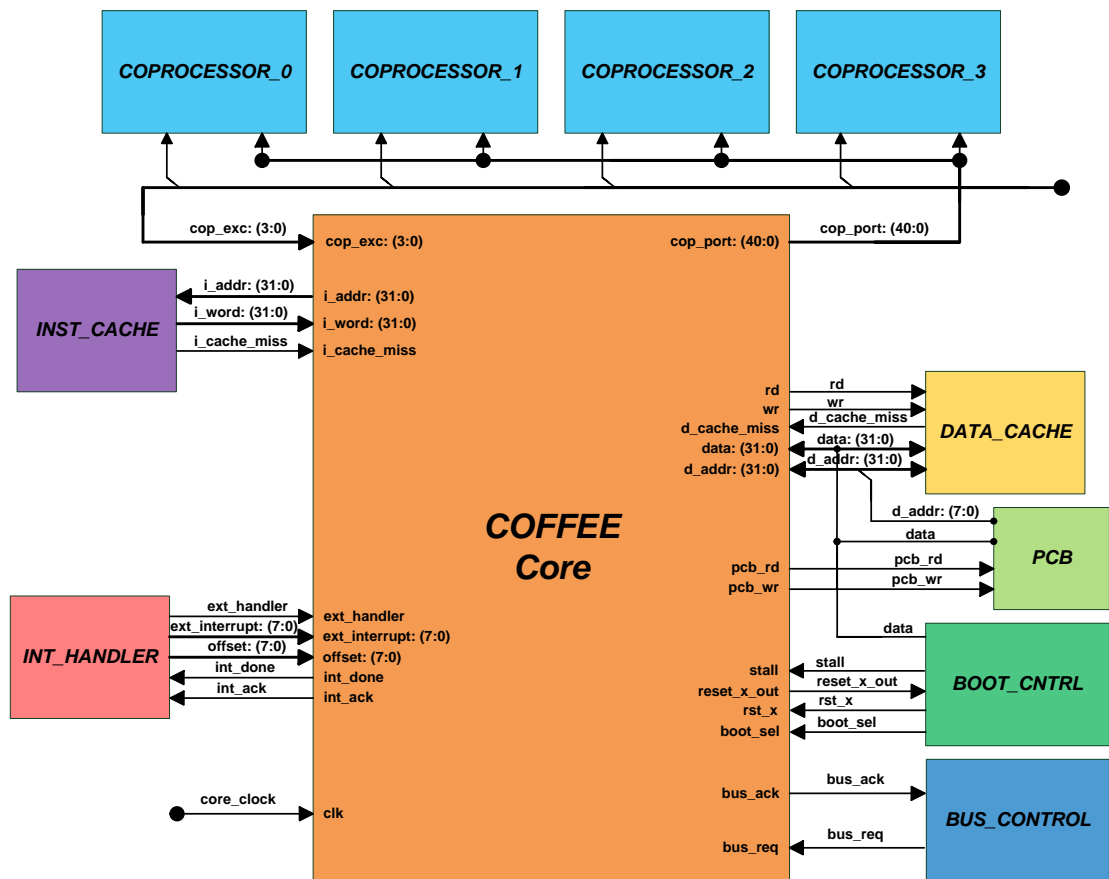


Figure 3.1: COFFEE core interface ©IEEE, 2003 [19]

3.1.2 Registers and Timers

The COFFEE has two register sets namely as SET1 and SET2 where each set consists of 32 registers including both general purpose registers (GPRs) and special purpose registers (SPRs). Application programs can use the SET1 but not SET2 whereas the privileged software (OS) can use both the SET1 and SET2 register sets. In addition to this, there are also condition registers (CRs) visible both to the

application programs as well as to the privileged software and they are 8 in total. The condition registers are used in case of conditional branches or when instructions are executed conditionally.

There is also an important register bank called Core Control Block (CCB) which is memory mapped and contains both the control as well as the status registers used in the processor operations. The advantage of being memory mapped is the access to them using general load and store instructions and can be configured using boot code. Most of the registers in these two sets are 32 bits wide with the exception of one named as Processor Status Register which is 8 bits wide. The detailed description of the Core Control Block registers like their addresses in memory, their usage and bit fields of the status register can be found in the user manual of the COFFEE core.

As far as timers are concerned, COFFEE has two independent 32-bit timers that can be configured to operate as a timer tick generator or as a watchdog timer. By default, these timers use the same clock frequency as the core itself. Otherwise there is an option called pre-scaling which can scale down the operating frequency of these timers. The pre-scaling registers are 8 bits wide and can be accessed using the same load and store instructions besides other registers like timer configuration register, register to hold maximum count and of course a free running timer register. The timers can be enabled/run or stopped, continuous or go for once, generate an interrupt on reaching a maximum count and also act as a watchdog timer to reset the core in-case the core gets stuck somewhere. Again, refer to the user manual for complete understanding of the timer registers and the options available for the application developer.[20]

3.1.3 Operating Modes

Generally there are two modes of operation for the COFFEE core namely as super user mode and user mode. In super user mode, the core can access the full memory space along with both the register sets whereas in user mode, as stated earlier, only first register bank is accessible. The user can switch from super user mode to user mode but not vice versa unless a specific instruction is used which transfers the

execution to the system code. The core boots initially in the super user mode so as to configure itself properly by accessing the core control block (CCB) registers and then transfers control to the user mode.

There is a start-up sequence which needs to be followed while powering-up the system like when the core powers up, the reset pin should be pulsed low to set the core in the correct state. Also if the boot address selection is enabled, the data bus should be provided with the boot address with the reset signal, otherwise it will boot at address 0x00000000h. The core will boot in the super user mode (32 bits) where interrupts are disabled and all the CCB configuration registers are appropriately set followed by transfer of control to the user mode.[20]

3.1.4 Interrupts and Exceptions

COFFEE core supports a total of 12 external interrupt sources where 4 of them are reserved for coprocessors and the other 8 are for general purpose usage. In addition to this, an external interrupt controller can be connected to further increase the number of interrupt sources. The priorities for the coprocessor interrupts are software programmable but for the external 8 sources, it is fixed. Priority can be set by writing a 4-bit value in the corresponding field reserved for that source between 0 to 15, where 0 being the highest priority.

The interrupt is triggered by an interrupt signal and then it is serviced in the following manner. The actions performed are priority resolving, switching to an interrupt service routine and finally returning from an interrupt service routine. The interrupt handler registers are located in the Core Control Block (CCB) which includes the control and the status registers. Similarly for an exception handling, there are codes associated to those as well as the priorities of course.[20]

3.1.5 Core Pipeline Structure

COFFEE core consists of single pipeline with six stages where each stage performs some operation or data transformation during one clock cycle. The intermediate or final results are clocked to registers of successive stages and execution proceeds from left to right. As there are six stages in the execution pipeline, it takes six clock cycles

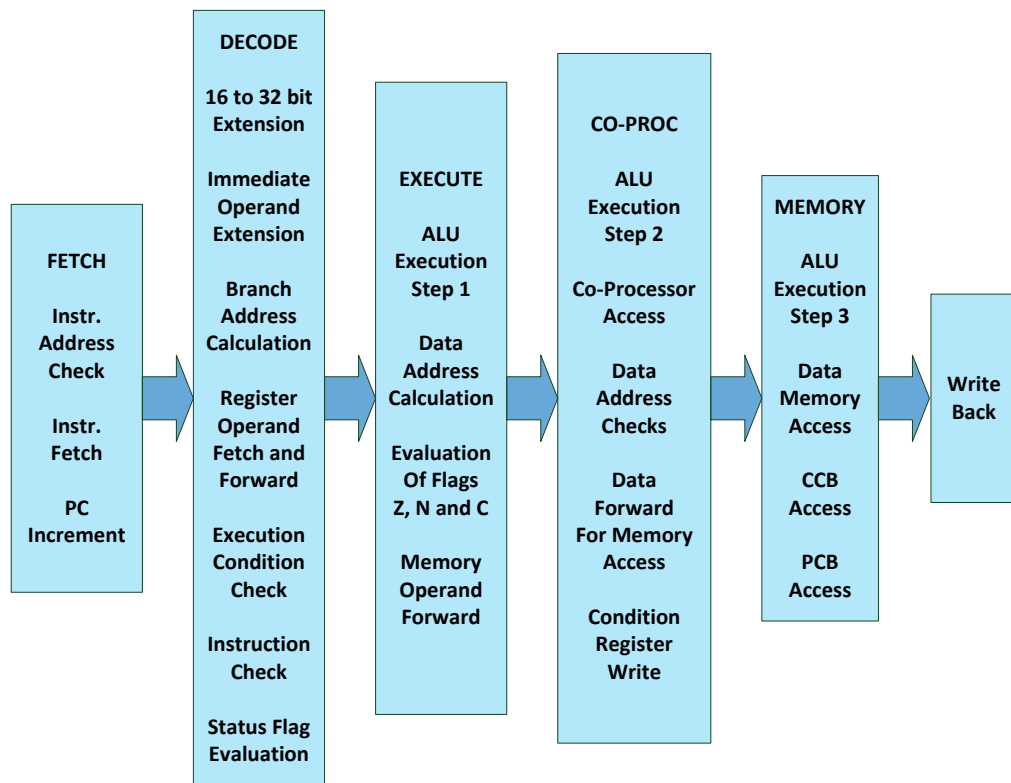


Figure 3.2: Core pipeline stages [21]

for an instruction to go through it. Ideally the throughput of the pipeline is one IPC (Instructions Per Cycle) without any stalls which means that every clock cycle, a new instruction enters the pipeline and one instruction completes its execution. The core pipeline stages are shown in Figure 3.2 and briefly described here as follows;

- Three operations are performed in the stage of FETCH. A new 32-bit instruction is fetched from the location pointed to by the program counter PC. A 32-bit double instruction is fetched if the address is even in 16-bit mode. An address in PC is checked which may lead to exception generation in case of violation. Depending upon the mode, program counter is finally incremented by two or four.
- From the control point of view, the DECODE stage is considered the most important. Instructions are identified and most of the decisions are made about their behavior in the next stages. If the decoding mode is 16-bit, 16-

bit halfword is extended to an equivalent 32-bit instruction before passing it to the decode logic. Special fields inside instruction word which define the execution condition are evaluated. In evaluation, pre-evaluated condition flags against the specified condition are checked. The instruction gets flushed on the next rising edge of the clock if execution condition is false. Signals required during the current and following stages are decoded from the instruction word simultaneously with the execution condition check. The control checks for data dependencies based on signals evaluated in DECODE stage and signals decoded from previous instructions currently on pipeline.

All data dependencies are resolved by forwarding the required data as soon as it becomes available. FETCH and DECODE stages are put to STALL if data cannot be forwarded and remain in this state until data becomes available. Support of hardware to resolve dependencies makes programming and compiler construction easier. The forwarding logic has approximately a delay of one-third of a clock cycle which does not reduce the clock frequency but rather improves the performance by avoiding unnecessary stalls.

Extending immediate operand, calculating PC relative jump address and evaluating new status flags if needed are also other operations performed in DECODE stage. At the end of the stage, the target address is clocked into the PC register. In DECODE stage, all jump instructions and conditional branches (PC relative and absolute) are executed. Register operands whether forwarded or fetched from register file are clocked to input registers of the EXECUTE stage.

- Data is manipulated in the EXECUTE stage and integer addition, shifting, boolean and bit-field manipulating instructions are completed during this stage. All the multiplication operations started in this stage produce intermediate results to next stage. The ALU's adder is used to calculate the address for data memory access. Condition flags ($Z = \text{zero}$, $N = \text{negative}$, $C = \text{carry}$) are evaluated at the end of the cycle using compare and some of the arithmetic instructions.

- In the CO-PROC stage, instructions requiring more than one cycle continue to be executed. Multiplication of 16-bit operands which produces a 32-bit result finishes in this stage. The condition flags are written to selected condition register which were evaluated in the previous stage and are available for DECODE stage prior written to condition register bank. How this is achieved is by forwarding data inside condition register bank from input to output if the source register and target register are the same. Also in this stage, the data memory address calculated in previous stage gets checked along with address comparison against memory limits set for user. Memory access is not performed if the address points to the configuration block, CCB, which is also checked. All co-processors accesses are performed in this stage and address calculation overflow is detected too. Pipeline gets stalled during wait cycles in case a co-processor access takes multiple cycles and hence performance deteriorates unless special interface block is used.
- 32-bit multiplication instructions execution completes in this stage of MEMORY. Instructions like ld and st also complete their work during this stage by accessing data memory. In case of multi-cycle execution, the rest of the pipeline is stalled during wait cycles as MEMORY stage cannot be bypassed by the instructions coming behind. Hence fast data memory or data cache and prefetch capability are considered very important.
- Execution of all instructions gets completed in the last stage of Write Back producing data which is written to the selected destination register. Internal forwarding of register file makes data in this stage visible to DECODE stage.

COFFEE is an RTL (Register Transfer Level) soft core described using VHDL and can be ported to any technology with basic library components. The core was designed to be a general purpose processing element suitable for most applications in either SoC (System-on-Chip) environment or in more conventional embedded systems. Its basic version provides adequate resources and processing power for many applications but in various ways it can be enhanced. COFFEE core can be customized as it was designed to be easily modifiable and provides simple interfaces

for expansion and communication. It is easy to instantiate COFFEE core anywhere because of its simple interface. The main postulates for COFFEE core design were reusability and configurability and it is published as an open source component.[19]

3.2 NineSilica MPSoC Platform

In this section, introduction to the homogeneous MPSoC platform is provided. The functionality of computational cluster is introduced and other architectural mechanisms are described.

3.2.1 Introduction to the Platform

NineSilica is a homogenous MPSoC platform derived from the *Silicon cafe* template which allows creation of either homogeneous or heterogeneous architectures with an unlimited number of computational nodes. This platform has been developed in the Department of Electronics and Communications Engineering, Tampere University of Technology. The platform contains nine computational clusters (CCs) connected to each other in a mesh topology through a hierarchical Network-on-Chip. The template does not define the type of processing element (PE) inside the computational cluster hence allowing creation of heterogeneous systems.

The nine computational clusters are organized in such a manner that there are three computational clusters on each side of the square with the ninth one in the center acting as the master on the NoC. The master CC is equipped with I/O peripherals and it can access all the CCs using the well defined routing procedure. The master CC's main responsibility is to manage the communication between slave CCs and to control their activities. The Master CC manages the schedule by distributing individual tasks to slave CCs to achieve parallelism and coordinates communication with them. The central position of the Master CC is important in a sense that it ensures a balanced latency across all slave CCs with maximum hop count of 2 in between any slave and itself.[18] The NineSilica MPSoC platform is illustrated in Figure 3.3.

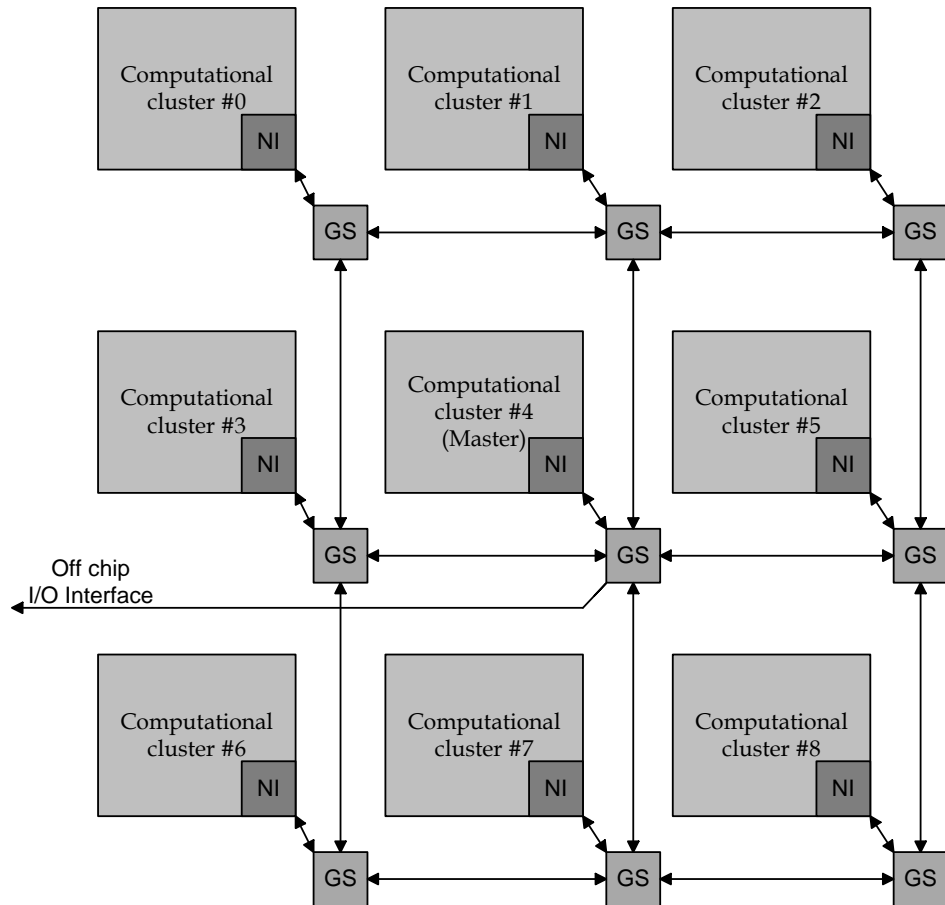


Figure 3.3: NineSilica MPSoC platform ©IEEE, 2009 [18]

3.2.2 Network-on-Chip (NoC)

Network-on-Chip as the name suggests is a communication network inside a single chip and allows mostly PEs to be inter-connected. There is a local level of hierarchy which provides non-blocking connections between processing core and its peripherals forming a single node. The communication between nodes is enabled by a global level of hierarchy via a mesh network. Based on the traffic conditions, the interconnection routes can be adapted at run-time. A lookup table with 16 possible routing paths are available to each NI for the communication over the NoC. During a remote write request from the local processor, 4 bits of the data address are used for the entry value of the lookup table.[22]

3.2.3 Computational Cluster

The computational cluster is composed of COFFEE RISC core, scratchpad type data and instruction memories (IMEM and DMEM) and a NI to latch together the internal communication structure to NoC. Regarding the individual processing node, a network interface is provided to each of the computational clusters (CCs) composed of a bridge that allows the CC to write data using the NoC. The bridge is responsible to latch together the global network communication with the communication inside a computational cluster. In each CC, there are two contending initiators, one is the processor itself and the other one is initiator side of the bridge (B/I). The idea is that each CC has to use the global switch to interact with the rest of the CCs. Processor can access the remote peripherals of another cluster by the local switches to the target side of the bridge (B/I). The computational cluster is shown in Figure 3.4.

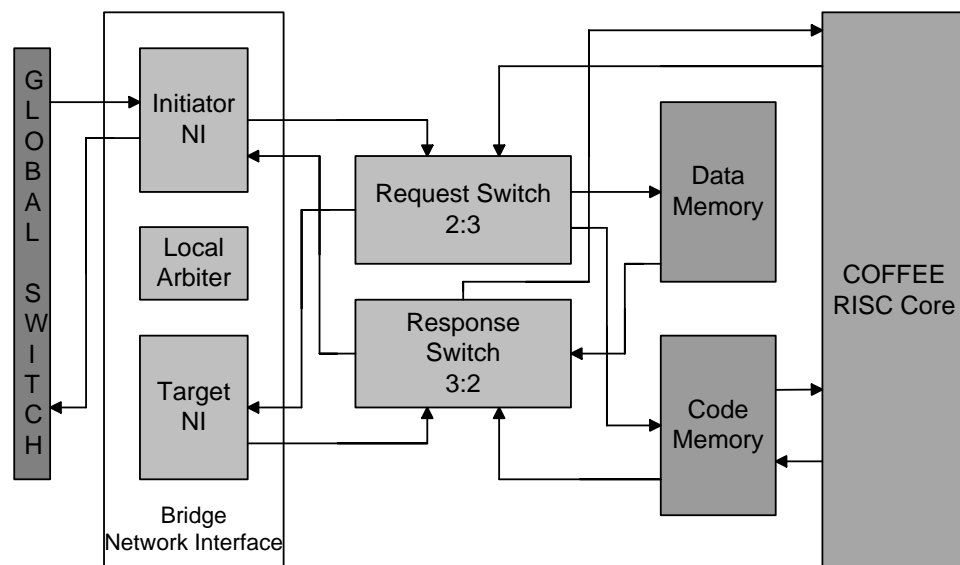


Figure 3.4: Single computational cluster ©IEEE, 2009 [18]

The receiving computational cluster includes the target side of the bridge interface (T-BIF), the local data memory and the local instruction memory of scratch pad type. A run-time reconfigurable source routing table is used to pick up the route to the destination address by T-BIF. Currently a total of 16 different routes can be configured and these routes are assigned to fixed size memory pages. This commu-

nication infrastructure supports both multicasting and broadcasting besides point to point communication between the central node and any of the other slave nodes. Each computational cluster hosts COFFEE RISC core as a PE due to its internal architecture.

3.2.4 MPSoC Platform for SDR Applications

NineSilica is a homogeneous MPSoC platform in which the number of nodes are kept at nine in order to limit the latency of data distribution and hence the communication overhead. Because of the mesh topology, it was decided to use nine nodes where there is one control node and all the others are processing nodes. This is how the intra-cluster data distribution requires only 1-2 hops and there is a uniform distribution of workload among the processing nodes. To execute remote read and write operations, a distributed shared memory approach has been chosen where each PE can write on a peripheral like data memory, instruction memory or network interface. Direct read operation is not supported to avoid possible data races due to remote read of an outdated variable. There is a shared space used for synchronization and exchanges of addresses of remote variables. Read operations are performed as write request to the remote cluster where the cluster updates the value in the shared variable. Also the data coherence is maintained at application level by the application developer as COFFEE RISC core is cacheless. Communication protocols like shared memory and message passing can be implemented efficiently on this platform.

Regarding the performance of the platform if we consider the applications mapping, the speedup close to the theoretical limits of N (number of nodes) can be achieved. All this is made possible because of the scalability which has often been attributed to the broadcast and multicast support of the hierarchical NoC. From the application developer's view point, the platform is programmable in C language and every node has its own instruction memory from where the local PE executes the program instructions. Generally a couple of C code files are prepared, one for the master core and the other one for all the processing cores. There is no need to write N code files for each of the available processing nodes due to logical division of the platform into

control node and processing node. Each processing node is identified by a unique ID which is assigned at run-time by the control node hence processing nodes application partitioning can be parameterized according to their IDs. The software written for the control node is mostly responsible to initialize the platform and maintaining the synchronization among the cores while executing the application software. Based on the assigned IDs, individual processing nodes identify their responsibilities along with the data set to operate on, number of data exchanges to be made and status and control flags communications.[22]

3.2.5 Communication and Synchronization

For real world communications, the control node is provided with I/O interfaces. Considering baseband signal processing applications, the control node receives data from outside world and distributes them to processing nodes for further computations. For inter-node communications, 32-bits are reserved to route the data packet to the intended peripheral like DMEM, IMEM or NI. Control node assigns IDs to individual processing nodes followed by sharing of synchronization signals as a part of initialization of the platform. The processing nodes follow instructions from control node before starting any process either computation or communications. Once the required data is made available to all the processing nodes, control node then sends them a control signal to initiate the computation process. Upon completion of the assigned task, each of the processing nodes asserts the status signals such that the control node can proceed for further actions. Finally the processing nodes are asked to transfer the computed results back to the control node. Based on this flow of execution, the control node of the platform acts as tasks scheduler and controls the task distribution among the processing nodes. Addressing schemes like point-to-point communications, multicasting and broadcasting are also supported in this architecture. If data is to be transferred to all the processing nodes, using broadcasting mode of communications can save almost 30% of the time.[22]

Table 3.1: Stratix II synthesis results of NineSilica MPSoC ©IEEE, 2009 [18]

Component	Adapt. LUT	Registers	Utilization %
COFFEE RISC	7,862	4,945	7.5
Local network node	346	232	0.3
Computational node	8,237	5,177	8
Global network	2,813	3,548	3
Total	76,780	50,482	73

Table 3.2: Stratix IV synthesis results of NineSilica MPSoC ©IEEE, 2010 [23]

Component	Adapt. LUT	Registers	Utilization %
COFFEE RISC	7,054	4,941	2.0
Local network node	296	226	0.1
Computational node	7,360	5,167	2.1
Global network	5,104	4,170	1.3
Total	71,679	50,897	20

3.2.6 Hardware Implementation

The synthesis results of this MPSoC platform on an Altera Stratix II FPGA device (EP2S180) as well as on Altera Stratix IV FPGA device (EP4SGX530) are reported in [18][23]. The operating frequency in fast mode is reported as 180MHz whereas in the case of Stratix II device, the maximum operating frequency reported is 75MHz. The synthesis of the platform has been made using the Quartus II version 8.0 SP1 design flow. If we compare the synthesis results of Table 3.1 and Table 3.2, the amount of resources occupied is roughly the same for both the cases but as far as hardware resources are concerned, the design on Stratix IV device utilized only 20% of the available resources as it is a larger platform. The architecture runs at a frequency of 115MHz in the FPGA slow mode.

NineSilica is a flexible and scalable platform which provides instantiated tiles of the same nature for mapping varying nature of applications. By carefully identifying the requirements, inherent parallelism can be exploited to achieve better performance outcomes. Maximum performance can be obtained by minimizing the unnecessary overhead and by proper planning of task distribution.

4. ALGORITHMS MAPPING

A typical baseband receiver executes digital signal processing algorithms to extract the bit stream transmitted from source equipment. To test the functionality of the baseband algorithms, a random sequence of symbols are generated using selected constellation and performed the necessary physical layer procedures according to 3GPP (FDD) and IEEE 802.11a specifications. Pulse shape filtering is applied to the generated signal and then distorted by using simple channel model which adds multipath taps and average white gaussian noise to the signal. The signal is then filtered again with the receiver version of the pulse shape filter and saved in an array that serves as an input to the receiver. All these operations have been performed using MATLAB software to generate the input test stream for the receiver such that it can perform the baseband operations.

4.1 WCDMA Parameters

The constellation used for this experimental work is QPSK and the Signal-to-Noise (SNR) ratio of 25dB. The transmission slots for WCDMA is 15 within a single frame of 10ms duration. The chip rate is 3.84MHz and the maximum length of the channel delay spread is 1024. The relative delays of multipath components are also set with the corresponding number of rake fingers which is 4. The Spreading Factor (SF) is 32 and the Pseudo-random (PN) sequence is generated using scrambling code number of 512. The Dedicated Physical CHannel (DPCH) is formed using Dedicated Physical Data CHannel (DPDCH) and Dedicated Physical Control CHannel (DPCCH). Control and data information are multiplexed on each one of the DPCH slots forming a complete frame of 10ms duration. The control information includes Transmit Power Control (TPC), Transport Format Control Indicator (TFCI) and PILOT symbols altogether form a DPCCH channel. The DPDCH consists of data symbols transmitted within each slot of DPCH defined as DATA1 and DATA2 fields

as shown in Fig 2.6. The DATA1 field consists of 14 symbols, DATA2 of 56 symbols, TPC of 2 symbols, TFCI of 4 symbols and PILOT consists of 4 symbols altogether result in 80 symbols. Hence a complete frame of DPCH composed of 1200 symbols finally gets modulated by performing the operations of spreading and scrambling. Common Pilot CHannel (CPICH) is also used such that the receiver can perform the operation of multipath estimation. CPICH is also spread using a SF of 256 and scrambled using the same PN sequence.

4.2 WCDMA Baseband Processing

The WCDMA receiver baseband signal processing involves multipath estimation, demodulation, channel estimation and symbols demapping algorithms execution. The software implementation of WCDMA baseband algorithms for NineSilica platform are described here as follow;

4.2.1 Multipath Estimation

The multipath estimation kernel has been implemented in a way that in the beginning it detects the first multipath peak. In order to perform this operation, CPICH is used as a reference pilot sequence. CPICH is spread using a spreading factor of 256 and scrambled using a PN sequence. The PN sequence has been generated by using M-sequences with the scrambling code number of 512. The NineSilica's control node transfers this received sequence of pilot symbols to all the processing nodes. The DPCH is spread using a spreading factor of 32 and scrambled using the same PN sequence. These data symbols are also transferred to processing nodes after the coefficients. Once every processing node has got these sequences, they start performing correlation operations. After the completion of correlation operations, each of the processing nodes return the computed outputs to the control node. The control node then starts searching for the correlation peak by comparing the correlation outputs with the preset threshold value. When the control node finds a correlation peak, it broadcasts its index value corresponding to the first peak to all the processing nodes. The processing nodes then start to compute more correlation operations inside the tracking window. The sliding correlation operation is

performed between the received data and the known pilot sequence using the first peak index as a starting point. The correlation output is averaged over a number of slots and again these results are transferred to control node. The control node then finds the other three correlation peaks from the averaged correlation outputs as we have a total of four rake fingers in the receiver.

4.2.2 WCDMA Demodulation

Once the receiver has information about multipath components, the rake fingers can be configured according to their delay profiles. The detected multipath components define the starting times of four different received data sequences. The locally generated despreading signal needs to be synchronized for each of the detected multipath components. The demodulation operation is performed by despreading and descrambling the multipath components using the time-aligned despreading waveform. The spreading factor we have chosen for this experimental work is 32, which corresponds to 80 symbols transmitted per slot. As there are 15 slots in each WCDMA frame, so in total we have 1200 symbols per frame. There are four rake fingers in the rake receiver, hence each of the processing nodes correlates 150 symbols for each one of the rake fingers. The starting index value for correlation corresponds to the multipath component detected in multipath estimation. Each processing node despreads and descrambles 600 symbols in total and thus the eight cores perform these operations on 4800 symbols.

4.2.3 Channel Estimation

Channel estimation has been performed using the time-multiplexed DPCCCH channel pilot symbols. As stated already in the previous paragraph that there are 80 symbols transmitted per slot. From these 80 symbols, 70 symbols are reserved for user data and other 10 symbols are used for control information. From these 10 symbols, 4 symbols per slot are used as pilot symbols. The received pilot symbols need to be extracted from the output of each rake finger. These recovered pilot symbols are correlated with the known pilot symbol sequence for each slot. Hence the preliminary channel estimates can be computed for the slot in question. The

individual contribution of signal components are combined such that the SNR of resultant signal is maximized. The extracted symbols from the rake fingers are then combined and scaled with estimated phase and magnitude of the propagation path. Finally, the data symbols are extracted from these combined symbols. The NineSilica's control node transfers the demodulated data to all the processing nodes. Each of the processing nodes processes 160 symbols except the last node which processes 80 symbols. Because of fifteen slots in a frame, each processing node operates on a couple of slots but the last node operates on the fifteenth slot and that is how channel estimates are computed and data symbols are extracted.

4.3 OFDM Parameters

The constellation type chosen to generate the OFDM symbols is QPSK with the SNR of 25dB. Number of OFDM symbols used in the simulation are 15 and a simple Additive White Gaussian Noise (AWGN) channel is used. The length of an OFDM symbol is $4\mu\text{s}$ which is composed of a signal part as well as a cyclic prefix part. The signal part is of $3.2\mu\text{s}$ duration whereas the prefix part is of $0.8\mu\text{s}$ duration. The number of data symbols within a single OFDM symbol is 48 and there are 16 cyclic prefix symbols which altogether result in 64 symbols. The signal's bandwidth of 20MHz is divided into subcarriers with spacing of 312.5KHz which yield in 64 subcarrier frequencies of which 52 subcarrier frequencies are used for modulation. Four of the subcarrier frequencies are used for pilot symbols and the zero frequency signal is not used. To generate the OFDM WLAN packet, training sequences are generated for packet's preamble as per IEEE 802.11a standard. Having generated the short and long training sequences for the packet preamble, the random data symbols are generated for each of the OFDM symbols. As there are 15 OFDM data symbols specified for this experimental work, each of the OFDM symbols consists of 48 data symbols which results in 720 data symbols for the entire OFDM packet. Finally the signal is modulated using Inverse Fast Fourier Transform (IFFT) and then the cyclic prefix is added to each of the OFDM symbols to compose a complete OFDM packet.

4.4 OFDM Baseband Algorithms Mapping

The OFDM baseband receiver pertaining to IEEE 802.11a WLAN standard performs the operations of symbol timing and frequency offset estimation, demodulation, channel estimation and symbols demapping. The software implementation of OFDM baseband algorithms for NineSilica platform are described here as follow;

Timing Synchronization

Due to high data rate and packet switched nature of WLAN systems, a "single-shot" synchronization procedure is used in which synchronization is acquired very quickly once the packet starts. There is a preamble in the start of every packet as shown in Figure 2.8 which facilitates the single-shot synchronization. The start of the packet is unknown to the receiver due to random access network, therefore the first task is to detect the start of the incoming packet. Hence, the main tasks which are performed in the beginning includes the packet synchronization and the symbol synchronization.

The first synchronization algorithm executed is the packet synchronization in which an approximate estimate of the incoming data packet is found. Several approaches to packet detection exist like received signal energy detection, double sliding window packet detection and using the structure of the preamble. I have used the preamble structure for packet synchronization and hence will explain it briefly here. Referring to Figure 2.9, there are 10 identical short training symbols where each one of them is 16 samples long followed by two identical long training symbols where each one is 64 samples long. To exploit the periodicity of the short training symbols at the start of the preamble, a delay and correlate algorithm is used. A crosscorrelation operation is performed between the received signal and a delayed version of itself where the delay z^{-D} is equal to the period of the short training symbols that is $D = 16$. The received signal energy is calculated to normalize the decision statistic during the crosscorrelation window.

Once the packet timing is known to the receiver, it starts finding the symbol timing

such that the Discrete Fourier Transform (DFT) of individual OFDM symbols can be calculated. The result of DFT is then used to demodulate the subcarriers of the individual symbols. To obtain symbol timing information, the receiver again uses the known preamble and performs the crosscorrelation operation. The received signal is crosscorrelated with the known reference like the end of the short training symbols or the start of the long training symbols.

4.4.1 OFDM Demodulation

To demodulate the subcarriers at the receiver, the reverse operation of Inverse Fast Fourier Transform (IFFT) is used which is referred to as Fast Fourier Transform (FFT). The output of the FFT contains N_s QPSK values which are then mapped onto binary values and decoded to produce binary output data. The computation of N -point FFT using the algorithms of radix-2, radix-4 and radix-8 has been presented in [24]. The performance evaluation has been made using the number of clock cycles consumed and based on the given results, radix-2 has been declared best in terms of speed-up achieved and parallelization efficiency. But when it comes to required clock cycles, radix-4 algorithm gives the best improvement for both the 64-point and 2048-point FFTs. In this research work, the hardware platform used to evaluate the performance of these FFT algorithms is NineSilica. The main processing element is COFFEE RISC core and the performance comparison between single-core and multi-core platforms is also provided. Regarding the OFDM WLAN demodulation, 64-point FFT operation is performed to recover the transmitted subcarrier frequencies. The implementation details along with the profiling results are very well explained in the given reference paper in this subsection.

4.4.2 Channel Estimation and Equalization

The channel estimation operation is performed using the long training sequence as the transmitted sequence is already known to the receiver. Before computing the channel estimation coefficients, the two identical training symbols are averaged. In the beginning, the pilots on the data subcarriers are extracted from the training sequence which are referred to as reference pilot symbols. All the processing nodes

perform this operation and extract equal share of pilot symbols from the total of 48. In this case, each processing node has 6 pilot symbols extracted from the reference long training sequence. After that, the received pilots on the data subcarriers are extracted and averaged. As there are two identical long training symbols transmitted which correspond to 96 pilot symbols in total. Each processing node extracts 12 samples from both the long training symbols where 6 of them are from each symbol and averages them. Now the processing nodes have both the reference pilot symbols as well as the received pilot symbols. Each processing node starts computing the channel estimates by taking the ratio of the reference pilot symbols to the received pilot symbols. After computing the channel estimates, each processing node transfers the results back to the control node.

The demodulated data symbols are equalized using the equalization coefficients obtained for each of the subcarriers. As there are 15 data symbols used for this experimental work and in each data symbol, there are 48 data samples modulated, therefore these 48 data samples for each of the data symbols need to be equalized using the computed channel estimates. In the beginning, the control node transfers the channel estimates to all the processing nodes followed by transferring the received data symbols. Each one of the processing node has been transferred a couple of data symbols except the last node which was provided with only one data symbol. Therefore each processing node equalizes 96 data samples except the last node which equalizes 48 data samples.

4.5 Symbols Demapping

To make decisions on the transmitted symbols for both the cases of WCDMA and OFDM baseband receivers, the decision boundaries determine how received symbols are mapped to bits. The maximum-likelihood decision is the constellation point that is closest to the received symbol. The computed raw data symbols need to be corrected by using the maximum-likelihood approach to determine the actual constellation points. In both the WCDMA and OFDM baseband receiver implementations, the transmitted data symbols are determined using the technique of

maximum-likelihood in which a relative distance between received symbols and one of the constellation points is calculated. The constellation point corresponds to the minimum distance was selected as a transmitted symbol.

Once the data symbols are extracted, each of the processing nodes starts making decisions on the recovered data symbols. The extracted symbols need to be demapped according to the constellation type used at the transmitting end. Quadrature Phase-Shift Keying (QPSK) modulation scheme has been used so there are four constellation points. The processing nodes find the transmitted symbols by computing the absolute distance between the recovered symbol and those four constellation points. For the case of WCDMA baseband receiver, each of the processing nodes demap 140 data symbols except the last node which processes 70 symbols. Finally, the demapped symbols are transferred to the central control node for further processing.

For the case of OFDM baseband receiver, after performing the operation of equalization, the processing nodes already have the data samples which can be demapped. All the nodes have 96 data samples except the last one which has 48 data samples. All the processing nodes perform the same operation on the recovered data samples and find out the actual transmitted constellation points. Once all the nodes are done with this process, they transfer back the final results to the control node. The processing nodes also determine the number of corrupted data samples by comparing the recovered data samples with the actual transmitted data samples. Finally the control node finds out the total number of erroneous samples as well as the Bit Error Rate (BER).

5. RESULTS

The algorithms have been implemented using C language with 16-bit fixed-point arithmetic. The results have been compared with the MATLAB model and functional correctness has been verified. For simulations purpose, the Mentor Graphics ModelSim simulator has been used. In the beginning, the algorithms have been mapped on the single core of COFFEE processor followed by implementation on NineSilica platform. The idea behind this experimental work was to exploit the parallelism offered by multicore systems and to evaluate the performance difference between single core and multicore platforms. Table 5.1 shows the profiling results of the WCDMA baseband algorithms implementation for both the single core and multi-core platforms.

The control node of NineSilica platform assigns individual processing nodes with their IDs in the system startup process so that they can identify their data sets to operate on and also compute the relative addresses to write back the results. In the system startup process, the control node broadcasts the base address of an array where all processing nodes write their final results. A synchronization signal is then asserted in the shared memory spaces of all the slave nodes so that they can acknowledge the reception of the transmitted information. The slave nodes then read the transmitted information like their IDs and assert the synchronization signals at

Table 5.1: WCDMA baseband algorithms profiling results ©IEEE, 2013 [25]

Algorithms	Single-core (clock cycles)	Multi-core (clock cycles)	Speedup
Multipath estimation	48,865,718	6,059,506	8X
Demodulation	4,467,747	575,723	7.7X
Channel estimation	581,195	144,440	4X
Symbol demapping	339,490	62,449	5.4X

their assigned addresses in the shared memory space of control node. This initialization (startup) process takes 656 clock cycles. The control node mostly remains in idle state when processing nodes are busy in computations or transferring data back to it. Depending upon the kernel being executed, number of inter-node communications may vary. In order to keep the workload balanced, the operations like correlations are divided equally among available cores such that maximum number of processing nodes have equal share of computations.

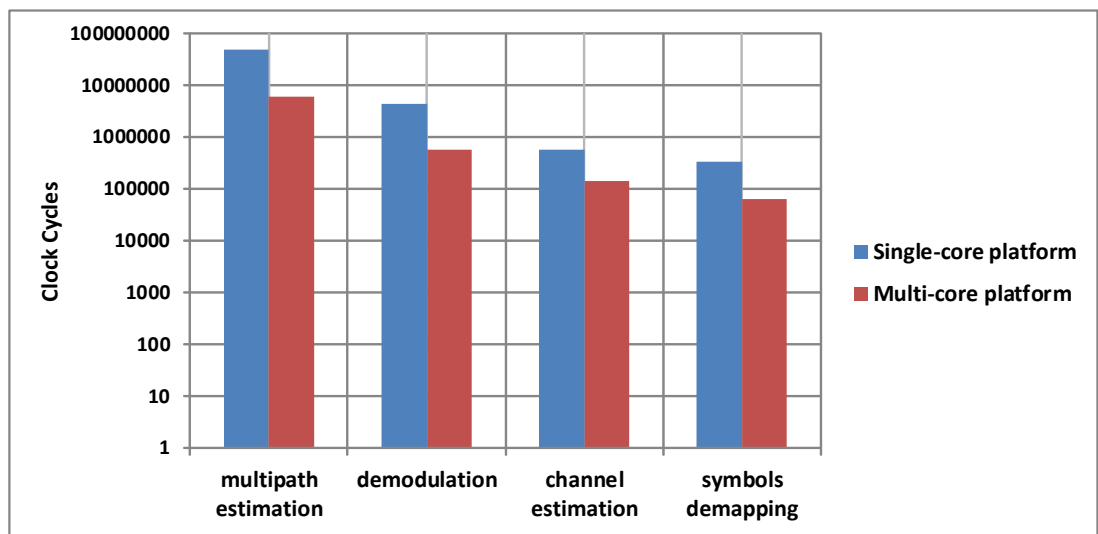


Figure 5.1: WCDMA baseband algorithms profiling results

There is a considerable performance difference between the two architectures as can be seen in Table 5.1. The profiling results are measured in terms of clock cycles consumed during the execution of an algorithm. Theoretically, an algorithm's execution time should be improved in accordance with the number of cores but practically it is not realistic. The fact is that sometimes the computational nodes are waiting for something to be completed by the control node before they can perform their job. For instance, the control node has to transfer the received data to all the processing nodes before they can start their computations. The bar chart is provided in Figure 5.1 to further illustrate the performance comparison between the two platforms. The execution performance is compared in terms of clock cycles which is given in

Table 5.2: OFDM WLAN baseband algorithms profiling results

Algorithms	Single-core (clock cycles)	Multi-core (clock cycles)	Speedup
Symbol timing and frequency offset estimation	5,514,850	1,118,383	4.9X
Demodulation ©IEEE, 2010 [24].	22,214	3,773	5.9X
Channel estimation and equalization	44,367	5,884	7.5X
Symbol demapping	175,227	22,375	7.8X

logarithmic scale.

In Table 5.2, the profiling results of OFDM baseband algorithms mapping on both the COFFEE core and the NineSilica platform are provided. The implementation results of OFDM demodulation algorithm were already available and details can be obtained from [24]. Based on the given results, the channel estimation and equalization and the symbols demapping algorithms achieved comparatively better speed-up than the other two kernels. Also the bar chart is provided in Figure 5.2 to analyse the performance comparison between the two architectures.

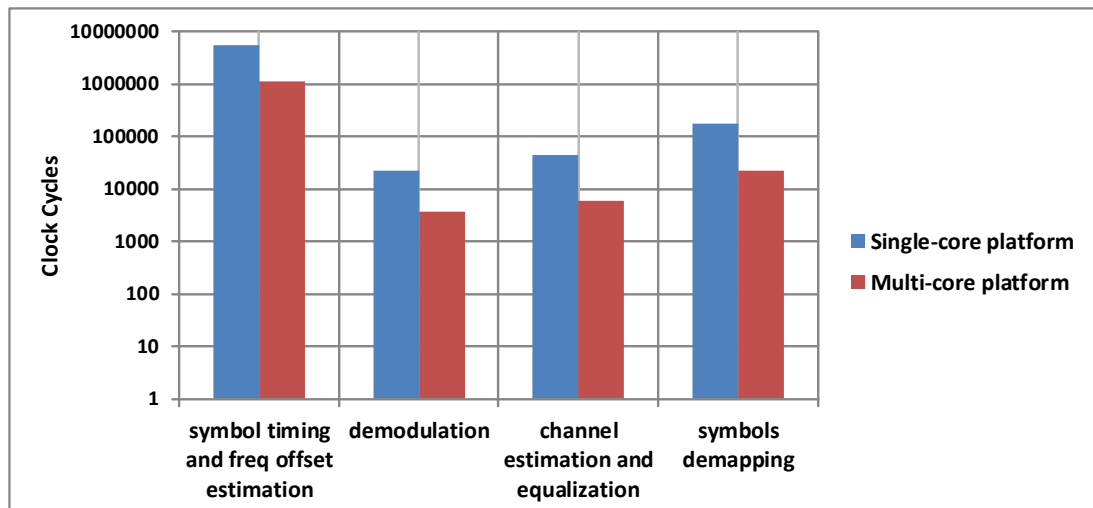


Figure 5.2: OFDM baseband algorithms profiling results

If we consider the bar charts for both the cases of WCDMA and OFDM baseband receivers, initial synchronization process seems to be the most time consuming part like multipath estimation kernel execution of WCDMA receiver and symbol timing and frequency offset estimation kernel for the case of OFDM receiver. Taking into account the real time requirements, each OFDM symbol should be processed in $4\mu\text{s}$ while for the case of WCDMA standard, each slot's duration is about $667\mu\text{s}$. Considering the synthesis frequency of 180MHz on an Altera Stratix IV FPGA device, the WCDMA baseband algorithms of multipath estimation, demodulation, channel estimation and symbols demapping took execution times of about 34ms, 3.2ms, 0.8ms and 0.35ms respectively. For the case of OFDM WLAN baseband algorithms like symbol timing and frequency offset estimation, demodulation, channel estimation and symbols demapping took execution times of 6ms, $21\mu\text{s}$, $33\mu\text{s}$ and $124\mu\text{s}$ respectively.

It is quite evident from the obtained execution times that the execution performance doesn't meet the real time requirements for both the standards. Considering the computational requirements of the algorithms, it is not possible for a general purpose processor to satisfy the strict timing requirements. From the hardware perspective, various steps can be taken to improve the performance like by increasing the number of processing nodes or by increasing the system clock frequency. Also hardware accelerators can be incorporated in the platform to satisfy the real time requirements like CGRAs, VLIW or DSP processors.

6. CONCLUSION

The performance of digital signal processors (DSPs) and general purpose processors has improved in the past many years along with reduction in their costs. But still the operational power is insufficient to meet the real time requirements of the wireless standards. Multiprocessor architectures are now becoming an important subject of the current research and are being considered as one of the prime candidates for wireless applications requiring computationally intensive tasks. In MPSoC platforms, performance is achieved by distributing or parallelizing the workload among available computational resources. Practical issues like distributing the algorithms among the processors besides task management and synchronization issues are of significant concern. Based on the hardware architecture, the proper allocation of resources is of utmost importance and it depends upon the functional requirements of the application. For instance, DSPs are good candidates to process high-speed signal processing algorithms while on the other hand CPUs are good for simple task control and management. The bottleneck to achieve real-time performance is the communication overhead between resources like CPUs and DSPs and the response times of interrupts. Multicasting and broadcasting mitigates the unnecessary communication overhead when nodes are connected in different communication topologies like using NoC or other general network communication schemes.

Based on the computational requirements of the most often used modulation schemes in wireless standards, manufacturers provided different options considering the market challenges. Multiprocessor platforms are one of the favorite candidates for this sort of applications and have proved themselves to be powerful computing engines. The complexity of wireless terminal implementation increases due to the multi-standard systems which demands for effective design methodologies. Tight time-to-market constraint can be tackled using programmable components and re-use of

existing standard software and hardware solutions. Real time requirements can be met using specialized or dedicated hardware accelerators within a single system-on-chip (SoC) design but meeting timing constraints using general purpose processors may require hundreds of processors if operated using lower frequencies. Using higher frequencies may lead to higher dynamic power consumption which is not very much recommended for embedded applications. Identifying the software and hardware requirements for multiple wireless standards can help tailor the SDR platform design and implementation of software components which can be re-used across different products.

In this thesis work, the baseband algorithms implemented for WCDMA standard are multipath estimation, demodulation, channel estimation and symbols demapping. For OFDM WLAN standard, the algorithms implemented are symbol timing and frequency offset estimation, channel estimation and symbols demapping. If we compare the performance differences between the single core and multi-core architectures, the WCDMA algorithms of multipath estimation, demodulation, channel estimation and symbols demapping achieved 8x, 7.7x, 4x and 5.4x speed ups respectively. While OFDM algorithms of symbol timing and frequency offset estimation, channel estimation and symbols demapping achieved the speed ups of 4.9x, 7.5x and 7.8x respectively. Considering the speed ups achieved for mapping individual baseband algorithms, WCDMA got an overall speed up of 6.3X while OFDM got an overall speed up of 6.5X. Taking into account the number of processing nodes of the platform, the overall speed ups achieved are close to theoretical maximum. The theoretical performance improvement cannot be achieved because of overheads like interrupts latencies and communication among resources. The scalability of the homogeneous MPSoC platform brings performance improvement by enabling concurrent execution of identical operations in the processing cores. The profiling data revealed that by using the NineSilica platform, performance improvements can be obtained by exploiting the platform's inherent parallelism.

REFERENCES

- [1] Ihmig, M., Herkersdorf, A., "Flexible multi-standard multi-channel system architecture for Software Defined Radio receiver," 9th International Conference on Intelligent Transport Systems Telecommunications,(ITST), 2009, pp.598-603, 20-22 Oct. 2009
- [2] Jalier, C., Lattard, D., Sassatelli, G., Benoit, P., Torres, L., "Flexible and distributed real-time control on a 4G telecom MPSoC," Proceedings of 2010 IEEE International Symposium on Circuits and Systems (ISCAS), pp.3961-3964, May 30 2010-June 2 2010
- [3] Garzia, F., Hussain, W., Airoidi, R., Nurmi, J., "A reconfigurable SoC tailored to Software Defined Radio applications," NORCHIP, 2009 , pp.1-4, 16-17 Nov. 2009
- [4] Wolf, W., Jerraya, A.A., Martin, G., "Multiprocessor System-on-Chip (MP-SoC) Technology," IEEE Transactions on Computer-Aided Design of Integrated Circuits and Systems, vol.27, no.10, pp.1701-1713, Oct. 2008
- [5] Beigne, E., Clermidy, F., Miermont, S., Vivet, P., "Dynamic Voltage and Frequency Scaling Architecture for Units Integration within a GALS NoC," Second ACM/IEEE International Symposium on Networks-on-Chip, 2008. NoCS 2008., pp.129-138, 7-10 April 2008
- [6] Jalier, C., Lattard, D., Jerraya, A.A., Sassatelli, G., Benoit, P., Torres, L., "Heterogeneous vs homogeneous MPSoC approaches for a Mobile LTE modem," Design, Automation & Test in Europe Conference & Exhibition (DATE), 2010, pp.184-189, 8-12 March 2010
- [7] Di Stefano, A., Fiscelli, G., Giaconia, C.G., "An FPGA-Based Software Defined Radio Platform for the 2.4GHz ISM Band," Research in Microelectronics and Electronics 2006, Ph. D., pp.73-76.
- [8] Holma, H. and Toskala, A. , WCDMA for UMTS: Radio Access for Third Generation Mobile Communications, Copyright 2000, John Wiley and Sons Ltd, Baffins Lane Chichester, West Sussex, PO19 1UD, England.
- [9] Tanner, R. and Woodard, J. , WCDMA:Requirements and Practical Design, Copyright 2004, John Wiley and Sons Ltd, The Atrium, Southern Gate, Chichester, West Sussex, PO19 8SQ, England.
- [10] Richardson, A., WCDMA:Design Handbook, Copyright 2005, Cambridge University Press, The Edinburgh Building, Cambridge CB2 8RU, UK.

- [11] Harju, L., Nurmi, J., "Hardware platform for software-defined WCDMA/OFDM baseband receiver implementation," *Computers & Digital Techniques, IET* , vol.1, no.5, pp.640-652, Sept. 2007
- [12] Harju, L., Nurmi, J., "A baseband receiver architecture for UMTS-WLAN interworking applications", *Proceedings. ISCC 2004. Ninth International Symposium on Computers and Communications, 2004.*, vol.2, pp. 678- 685, 28 June-1 July 2004
- [13] Grayver, E., Frigon, J.-F., Eltawil, A.M., Tarighat, A., Shoarinejad, K., Abbasfar, A., Cabric, D., Daneshrad, B., "Design and VLSI implementation for a WCDMA multipath searcher," *IEEE Transactions on Vehicular Technology*, vol.54, no.3, pp. 889- 902, May 2005
- [14] Bastug, A., Montalbano, G., Slock, D., "Common and Dedicated Pilot-Based Channel Estimates Combining and Kalman Filtering for WCDMA Terminals," *Conference Record of the Thirty-Ninth Asilomar Conference on Signals, Systems and Computers, 2005.*, pp.111-115, Oct. 28 2005-Nov. 1 2005
- [15] Taewon Hwang, Chenyang Yang, Gang Wu, Shaoqian Li, Li, G.Y., "OFDM and Its Wireless Applications: A Survey," *IEEE Transactions on Vehicular Technology*, vol.58, no.4, pp.1673-1694, May 2009
- [16] Heiskala, J. and Terry, J. , *OFDM Wireless LANs: A Theoretical and Practical Guide*, Copyright 2002 by Sams Publishing, SAMS, 201 West 103rd St., Indianapolis, Indiana, 46290 USA.
- [17] Supplement to IEEE Standard for Information Technology - Telecommunications and Information Exchange Between Systems - Local and Metropolitan Area Networks - Specific Requirements. Part 11: Wireless LAN Medium Access Control (MAC) and Physical Layer (PHY) Specifications: High-Speed Physical Layer in the 5 GHz Band," *IEEE Std 802.11a-1999*, 1999.
- [18] Garzia, F., Airoldi, R., Ahonen, T., Nurmi, J., Milojevic, D., "Implementation of the W-CDMA cell search on a MPSOC designed for software defined radios," *IEEE Workshop on Signal Processing Systems, SiPS 2009*, pp.030-035, 7-9 Oct. 2009.
- [19] Kylliainen, J., Nurmi, J., Kuulusa, M., "COFFEE - a core for free," *Proceedings. International Symposium on System-on-Chip, 2003.*, pp.17-22, 19-21 Nov. 2003
- [20] http://coffee.tut.fi/docs/COFFEE_Core_USER_MANUAL.pdf

- [21] COFFEE RISC Core, website: http://coffee.tut.fi/docs/COFFEE_pipeline.pdf
- [22] Airoldi, R., Ahonen, T., Garzia, F., Milojevic, D., Nurmi, J., "Implementation of W-CDMA Cell Search on a Highly Parallel and Scalable MPSoC", *Journal of Signal Processing Systems for Signal, Image and Video Technology*, Springer US, Vol.64, Issue 1, 2011, pp.137-148.
- [23] Airoldi, R., Garzia, F., Anjum, O., Nurmi, J., "Homogeneous MPSoC as base-band signal processing engine for OFDM systems," *International Symposium on System on Chip (SoC)*, 2010, pp.26-30, 29-30 Sept. 2010
- [24] Airoldi, R., Garzia, F., Nurmi, J., "FFT Algorithms Evaluation on a Homogeneous Multi-processor System-on-Chip," in *Proc. International Symposium on Multicore Systems-on-Chip (MCSoc 2010)*, San Diego, CA, USA, September 13-16, 2010.
- [25] Fazal, Rizwan., Hussain, Waqar., Ahonen, Tapani., Nurmi, Jari., "Evaluation of WCDMA receiver baseband processing on a Multi-Processor System-On-Chip," *18th International Conference on Digital Signal Processing (DSP)*, 2013, pp.1-7, 1-3 July 2013